THESIS FOR THE DEGREE OF DOCTOR OF PHILOSOPHY

Development of novel bioanalytical assays with single-molecule readout for biomarker detection and drug candidate characterization

OLOV WAHLSTEN

CHALMERS

Department of Physics
CHALMERS UNIVERSITY OF TECHNOLOGY
Göteborg, Sweden 2017

Development of novel bioanalytical assays with single-molecule read-out for biomarker detection and drug candidate characterization

OLOV WAHLSTEN
ISBN 978-91-7597-606-8

Doktorsavhandlingar vid Chalmers Tekniska Högskola
Ny serie nr 4287
ISSN 0346-718X

Department of Physics
Chalmers University of Technology
SE-412 96 Göteborg
Sweden
Telephone +46(0)31 - 772 10 00

Printed at Chalmers Reproservice
Göteborg, Sweden 2017

Cover illustration: *(Left) A surface-based method where the interaction between individual membrane receptors, residing in fluorescently labeled native membrane vesicles, and immobilized ligands can be studied at a single-molecule level. By adding drug candidates, inhibiting the interaction at the surface, useful information can be extracted about the interaction between the drug and the membrane receptor. (Right) A solution-based method for detection of virus particles by colocalization of ganglioside-containing fluorescently labeled liposomes.*

Development of novel bioanalytical assays with single-molecule readout for biomarker detection and drug candidate characterization

OLOV WAHLSTEN
Department of Physics
Chalmers University of Technology

Abstract

Bioanalytical assays with single-molecule readout for studying molecular interactions have in the past decades received increasing attention. The high sensitivity often offered by this readout scheme has for example enabled ultra-sensitive analyte detection, having important implications for monitoring early disease progression and the effects of drug treatment. In addition, single-molecule studies of molecular interactions with membrane protein receptors have proven useful for the development of new and more effective drugs. Ultra-sensitive detection as well as the possibility to unravel heterogeneities in molecular interactions, offered by single-molecule readout schemes, are both key components for the future of personalized health care and the discovery of new disease biomarkers.

This thesis mainly focuses on the development of new bioanalytical assays with single-molecule readout, with the purpose to enable studies of molecular interactions with membrane protein receptors (an important class of drug targets) and to detect diagnostically relevant biomarkers and pathogens. Lipid assemblies, either in the form of liposomes or supported lipid bilayers, have been exploited for their compatibility and flexibility offered in the context of studying many essential biological interactions. In the first part of the thesis, two surface-based assays, both utilizing total internal fluorescence (TIRF) microscopy, were developed to study molecular interactions with a low-abundant and sensitive class of membrane proteins; G protein-coupled receptors (GPCRs). With the insights gained from that work, the focus was shifted towards solution-based detection schemes, based on a home-built dual-color fluorescence microscopy setup. Two detection schemes, based on Förster resonance energy transfer (FRET), for biomarker detection (phospholipase and miRNA), and a third scheme for detection of virus particles via induced colocalization of fluorescent liposomes, were developed.

As for future perspectives the thesis puts emphasis on how the different bioanalytical assays can have implications for personalized health care and how the performance of the solution-based colocalization assay can be further improved to become a generic tool for biosensing purposes.

Keywords: Bioanalytical assay, single-molecule readout, drug discovery, biomarker detection, fluorescence, liposomes, QCM-D, spectrofluorometry, TIRF microscopy.

Appended papers

Paper I:

Equilibrium-Fluctuation Analysis for Interaction Studies between Natural Ligands and Single G Protein-Coupled Receptors in Native Lipid Vesicles
Olov Wahlsten, Anders Gunnarsson, Lisa Simonsson Nyström, Hudson Pace, Stefan Geschwindner, and Fredrik Höök.

Langmuir **31**, 39, 10774-10780 (2015).

Paper II:

Cytomegalovirus Pentamer Complex-Dependent Engagement of the Endothelin B Receptor is Critical for Endothelial Cell Infection
Koon-Chu Yaiw, Tim Schulte, Olov Wahlsten, Abdul-Aleem Mohammad, Huanhuan L. Cui, Lisa Simonsson Nyström, Helena Costa, Vanessa Wilhelmi, Alice Assinger, Hudson Pace, Belghis Davoudi, Giorgos Tsipras, Patrick Scicluna, Natalia Landazuri, Masany Jung, Ourania Kostopoulou, Sharan Ananthaseshan, Suhas Vasaikar, Chato Taher, Lynn Butler, Afsar Rahbar, Hjalmar Brismar, Andrea Carfi, Jiri Bartek, Kum-Thong Wong, Per-Åke Nygren, Fredrik Höök, Adnane Achour, and Cecilia Söderberg-Nauclér.

Submitted.

Paper III:

High Sensitivity Detection of Phospholipase A2 Induced Lipid Mixing Using Dual-Color Fluorescence Imaging with Single Liposome Resolution
Olov Wahlsten, Björn Agnarsson, and Fredrik Höök.

Submitted.

Paper IV:

MicroRNA Detection by DNA-Mediated Liposome Fusion
Coline Jumeaux, Olov Wahlsten, Stephan Block, Eunjung Kim, Rona Chandrawati, Philip D. Howes, Fredrik Höök, and Molly M. Stevens.

Submitted.

Paper V:

Quantitative Detection of Biological Nanoparticles in Solution via Their Mediation of Colocalization of Fluorescent Liposomes
Olov Wahlsten, Frida Ulander, Björn Agnarsson, Daniel Midtvedt, Måns Henningson, Vladimir P. Zhdanov, and Fredrik Höök.

In manuscript.

Papers not included in the thesis

Paper VI:

Wounds as Probes of Electrical Properties of Skin
Olov Wahlsten and Peter Apell.

Journal of Electrical Bioimpedance **1**, 63-70 (2010).

Paper VII:

Physics of the Body Mass Index
Peter S. Apell, Olov Wahlsten, and Hanna Gawlitza.

Physics & Society **41**, 10-11 (2012).

Paper VIII:

Electrical Field Landscape of Two Electroceuticals
Olov Wahlsten, Jeff Skiba, Inder Makin, and Peter Apell.

Journal of Electrical Bioimpedance **7**, 13-19 (2016).

Paper IX:

Binding Kinetics and Lateral Mobility of HSV-1 on End-Grafted Sulfated Glycosaminoglycans
Nadia Peerboom, Stephan Block, Noomi Altgärde, Olov Wahlsten, Stephanie Möller, Matthias Schnabelrauch, Edward Trybala, Tomas Bergström, and Marta Bally.

Biophysical Journal **113**, 1-12 (2017).

Paper X:

Understanding Supported Lipid Bilayer Formation and Quality in the Presence of Non-ruptured Vesicles: A Study Based on QCM-D and TIRFM
Hudson Pace, Olov Wahlsten, Daniel Midtvedt and Fredrik Höök.

In manuscript.

Contribution to the appended papers

Paper I:

The concept was originally proposed by AG and FH. OW designed the study with support from AG, LSN and HP. The experiments were planned and performed by OW, who also analyzed the data. OW wrote the main part of the manuscript with input from all the co-authors.

Paper II:

The colocalization concept was developed by OW, LSN and FH. OW and LSN planned, optimized and performed the experiments. The data was analyzed by LSN. OW and LSN wrote the corresponding part of the manuscript with input from FH.

Paper III:

OW and FH designed the study. OW planned and performed the initial experiments for concept verification. OW performed the spectrofluorometer measurements. BA designed the dual-color microscopy setup with support from OW and supported OW in those measurements. OW wrote the image analysis scripts for PLA2 detection and used already established scripts for liposome size determination. The results were interpreted and the manuscript was written by all co-authors.

Paper IV:

OW, CJ, FH and PDH designed the microscopy study together. OW and CJ, planned and performed the relating experiments. The data analysis strategy was developed and performed by SB. OW assisted SB with additional measurements benchmarking the analysis strategy. OW wrote the part of the manuscript about the dual-color fluorescence microscopy instrumentation.

Paper V:

The detection mechanism was originally an idea of FH and OW. The experimental setup used was developed by BA with support from OW. OW designed, planned and performed the study with support from FU. OW and FU, with input from DM, developed the analysis scripts. OW developed the theoretical model together with MH and VPZ. OW implemented the theoretical model and wrote the main part of the manuscript.

Contents

1

Introduction

Biomolecular interactions occur in great numbers at every instant in our bodies and is a prerequisite for all life. Most biological processes are highly dependent on precise and timed interactions involving a plethora of biomolecules. These well-orchestrated interactions are essential for maintaining cellular homeostasis and in order for us to stay healthy. However, a slight dissonance among these biomolecular interactions or the presence of a few malevolent intruders (for example viruses or bacteria) can disturb this biological machinery and lead to disease. Being able to study interactions between biomolecules is thus important from many perspectives. Gaining deeper understanding of our biological complexity and diseases that can affect us are two apparent examples. In addition, biomolecular interactions are also important to study for developing new drugs and to learn more about biomolecular variations between individuals, which may have important implications for future personalized health care. However, it is not only the study of these biomolecular interactions that are of great relevance to the field of life science and medicine. So is also the ability to detect certain biomolecules (so called biomarkers), that might for example be indicative of a certain disease, in a specific and reliable manner. In fact, similar methods can be used to detect toxic or other harmful substances in for example food.

One of the most important and fascinating biological structures is the cell membrane, a barrier separating the cytoplasm from the surrounding aqueous environment, which encompasses transduction mechanisms to allow for communication across the membrane. These mechanisms can either relate to for example direct transport of nutrients or waste products or sensing of the external environment and conveying of the message into the cell, where a physiological response can be initiated. These sensing molecules, for example so called g-protein coupled receptors (GPCRs), are interesting targets for drugs[1]. However, GPCRs are low-abundant and their function is dependent on the lipid membrane environment in which they reside[2;3]. For this reason GPCRs are difficult to study because of their poor compatibility with conventional analysis methods, which often require that these membrane proteins are enriched by for example separation from the natural lipid environment or genetically modified to be more stable[4–7]. In **papers I** and **II**, surface-based platforms based on total internal fluorescence (TIRF) microscopy were developed to study interac-

tions with GPCRs, at a single-interaction level and with the GPCRs kept in a near-native environment.

While GPCRs due to their crucial functional role represent an important class of drug targets, the existence or changes in the expression level of many other types of molecules rather report on a disease state. The latter are often named biomarkers; a term coined back in the 1980's[8], which in its broadest sense refers to a measurable indicator of a physiological state of an organism. In the field of medicine, this indicator is usually a molecule whose expression level correlates with the progression of a certain biological process or disease. Two examples are the human chorionic gonadotropin (hCG) hormone produced by the placenta in pregnant women[9] and the prostate-specific antigen (PSA), a protein produced at elevated levels by the prostate gland in men with prostate cancer[10]. Additionally, biomarkers can be indicative of bacterial or viral infection. The discovery of new biomarkers is a constantly active research field, as is the continuous development of more and more sensitive diagnostic methods based on the specific detection of biomarkers. Other important aspects of the future of biomarker detection is the ability to detect multiple biomarkers in the same sample, in so called multiplexed assays. This is to give a better significance to the measured results as a disease state often alters the expression levels of multiple biomarkers, or several disease states may alter the expression level of the same biomarker. Further, the ability to detect biomarkers at very low concentrations and more convenient monitoring of concentration levels over time has important implications for early diagnostic and monitoring of disease progression after or during medical treatment.

With emphasis on offering simplified sample handling and readout, **papers III** and **IV** introduce solution-based assays developed for detection of two biomarkers; phospholipase A2 (PLA2) and the microRNA miR-29a, respectively. PLA2 is a biomarker for multiple disease states, including for example several types of cancer[11;12], acute pancreatitis[13], and ischemic stroke[14]. The miR-29a is a biomarker indicative of influenza virus infection[15]. Both assays rely on biomarker-induced mixing of fluorescently labeled lipids within liposomal structures such that readily detectable Förster resonance energy transfer (FRET) is induced.

The transition towards developing solution-based bioanalytical assays, although **papers I** and **II** were based on an utterly sensitive surface-based single-molecule concept, stems from the inherent hurdle of minimizing unspecific interactions with the underlying solid substrate and our interest in developing simple biosensors with few experimental steps and high success rate. In particular, **paper V** was developed as a reaction to **papers I** and **II**, in which significant efforts had to be invested in order to suppress non-specific interaction of native GPCR-containing vesicles and/or viruses with the underlying surface. Therefore, a concept that could potentially enable direct detection of virus particles in solution was developed. The proposed method is inspired by biomolecular assays that utilize dual recognition elements, targeting for example different epitopes of the analyte in a so-called sandwich format, offering highly selective detection. Representative examples are the well-established enzyme-linked immunosorbent assay (ELISA)[16] or assays based on analyte-

induced aggregation of colloidal particles decorated with the recognition elements[17–21]. Despite these concepts being developed several decades ago, recent efforts have been focused on methods to enable detection of individual sandwich complexes, with single-molecule resolution[22–28], thus improving the limit of detection. The method presented here takes advantage of aggregation of two different fluorescently labeled liposomes (red and green), containing the receptor for the virus, induced by the suspended virus particles. A dual-color fluorescence readout enabled detection of the early onset of the aggregation, and thus also a low limit of detection that makes the concept promising for future assay development.

The thesis has the following disposition: chapter 2 is meant to offer a biological foundation for the biological systems studied in this thesis. Chapter 3 is devoted to a historical perspective on biosensing including different sensing formats along with the possibilities offered by single-molecule sensitivity. Chapter 4 brings up and briefly describes central concepts and the main experimental techniques that have been used in this work. Chapter 5 summarizes the main results of the appended papers, and finally chapter 6 presents the concluding remarks and the future perspectives of the experimental assays that have been developed in this work.

2

Background

The central theme of this thesis work has been to detect and study biomolecular interactions. Therefore, the aim of this background chapter is to first elucidate the challenge of studying biomolecular interactions, that ideally resembles what occurs naturally, with conventional and established experimental techniques and readout principles. The integrity and function of many biomolecules is strongly dependent on the external environment, which inevitably necessitates careful consideration both when choosing experimental techniques and when interpreting the obtained results. Highlighted is also the importance of simplifying biological systems to make it possible to study individual interactions without having other factors inflicting and possibly distorting the outcome. On the other hand, oversimplifications of biological systems should also be avoided as a complete picture of a biological interaction is rarely fully unraveled using simple model systems. In addition to biological simplifications, other experimental strategies exploited for developing novel bioanalytical assays are briefly presented in this chapter.

As the majority of this thesis work relates to biomolecular interactions with the cell membrane, or with components residing in the cell membrane, a section is devoted to portray its features and importance for biological life. A speaking example of this is all the membrane proteins that reside in the cell membrane where they are responsible for many important functions, for example transport of nutrients and waste products across the membrane or communication between cells. As a matter of fact, as briefly mentioned previously, mimics of the cell membrane are often used to investigate interactions with the cell membrane. As a direct follow up on the section about the cell membrane a class of membrane proteins highly relevant for the pharmaceutical industry, namely G protein-coupled receptors (GPCRs), is presented. Surface-based platforms to study GPCRs were developed in both **papers I** and **II**.

The sections following the cell membrane and the GPCRs describes the individual biological components that were used in the remaining work to develop solution-based bioanalytical platforms. These are in order; A group of lipid-digesting enzymes named phospholipases (**paper III**), a microRNA sequence being a biomarker for influenza infection (**paper IV**), and virus-like particles (VLPs) of the Simian virus 40 (**paper V**).

2.1 Strategies for studying biomolecular interactions

In order to study complex processes occurring naturally inside our bodies, simplifications of the biological systems are often of great importance. The reason for this is that biological structures must be made compatible with the techniques used for the investigation and it is often an advantage if the studied entities or processes can be isolated from additional inflicting factors. Furthermore, being able to give the simplified model system a theoretical foundation may increase the relevance of the experimental results. Also, it is important to unravel the functions of isolated components before trying to figure out how additional functions arise from complex interactions with other components.

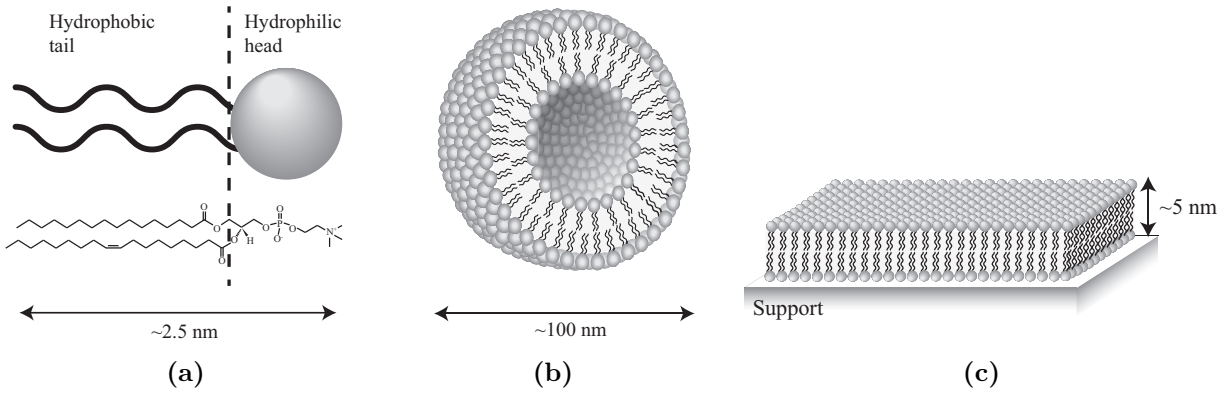

Figure 2.1: *An illustration of different lipid molecule assemblies. A single lipid molecule* ***(a)*** *is characterized by its hydrophilic head and hydrophobic tail(s). This amphiphilic nature is responsible for the self-assembly of lipid molecules into liposomes* ***(b)*** *in aqueous solutions and bilayers on solid supports* ***(c)****.*

In this thesis two common cell membrane mimics have been used; the liposome and the supported lipid bilayer. Many lipid molecules, illustrated in figure 2.1a, tend to spontaneously self-assemble into liposomes when dissolved in an aqueous solution, figure 2.1b. A supported lipid bilayer (SLB), illustrated in figure 2.1c, is formed spontaneously via liposome rupture on only a handful of surfaces (e.g. glass, silicon oxide, or mica)[29]. Variations in how these aggregates are formed exist due to varying physical properties of different lipids and surfaces. Bilayer formation via liposome rupture is often described by several concurrent processes: liposome adsorption, rupture of these liposomes when at a critical coverage leading to formation of bilayer patches, and merging of these growing patches to eventually form a complete bilayer[30;31].

In both surface-based assays, **papers I** and **II**, an SLB were used to passivate the surface and thereby minimize the amount of unspecific interaction with it. Importantly, not only the inert properties of the SLB was exploited, but also the possibility of attaching one of

the interacting partners on the surface. This could either be done via chemical bonding or exploiting self-insertion or anchoring into the hydrophobic interior of the SLB. To enable the molecular interactions occuring on the substrate (i.e. the functionalized SLB) fluorescently labeled lipid vesicles [†], holding membrane proteins (either naturally expressed or reconstituted), also function as signal enhancers that enable single-molecule interactions to be monitored.

In the solution-based assays, **papers III**, **IV** and **V**, liposomes were exploited both as fluorescent reporters and for functionalization. The interaction partner was then freely diffusing in solution and could be detected either by probing lipid mixing between the liposomes (**papers III** and **IV**) or simply liposome colocalization (**paper V**).

2.2 The cell membrane

The living cell is the smallest unit that is classified as being alive and ranges in size from 1 to 100 μm depending on cell type, see figure 2.2. Additionally, cells are considered the most complex systems of that size that we know of[32]. Since this thesis mainly focuses on direct studies of molecular interactions with components residing in the cell membrane, and on development of methods where biomolecular interactions with the cell membrane are exploited, the entire cell machinery and crowded interior of the cell is not further discussed. Instead focus will be on the cell membrane, artificially produced mimics of it and the importance of a specific class of membrane proteins when it comes to discovering certain new drugs.

The plasma membrane, enclosing the cell, has been of great importance in the formation of life. Despite a thickness of only $\sim 5\,\text{nm}$, it serves as a physical barrier to maintain essential differences in chemical compositions between the cell interior and exterior. However, the membrane must allow for transport of for example nutrients into and waste products out of the cell. Furthermore, to enable cell movement, growth and division, it is important that the plasma membrane is flexible. The solution that Nature has evolved to meet these requirements is to use a type of molecular building blocks with two distinct physical properties interconnected mainly by non-covalent interactions.

The amphiphilic phospholipid is one of the most abundant lipid species in cell membranes[33;34]. The Greek *amphis* means "both" and *philia* means "love". The molecule has both a water-loving (hydrophilic) part and one fat-loving (hydrophobic). These two properties are fundamental for molecules forming membranes. To minimize the free energy when dissolved in an aqueous solution the hydrophilic heads screen the hydrophobic tails and assemblies are formed spontaneously, which is referred to as *the hydrophobic effect*[35]. The optimal head-group area, critical chain-length and hydrocarbon volume of the

[†]Throughout this thesis *liposomes* refer to the hollow spherical assemblies of lipids or lipid conjugates, whereas *vesicles* might consist of other components as well, such as for example membrane proteins.

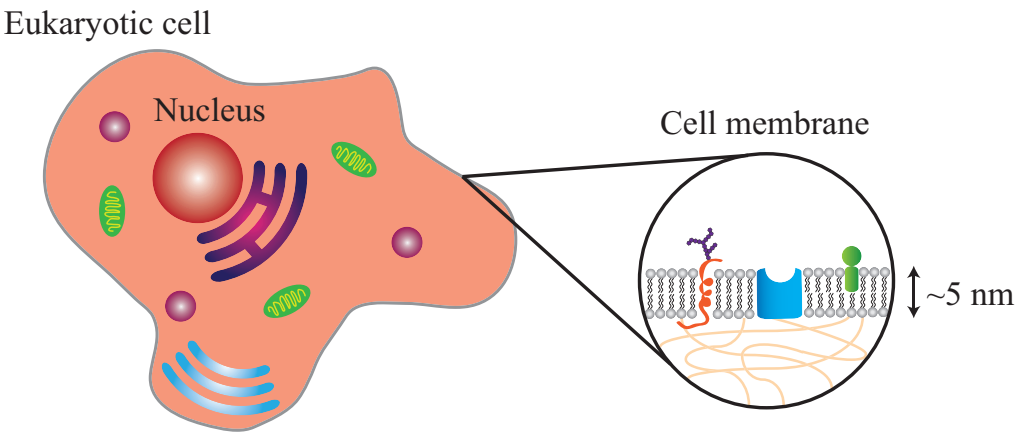

Figure 2.2: *An illustration of a eukaryotic cell, with cell nucleus and other organelles such as the golgi apparatus, lysosomes, endoplasmic reticulum and mitochondria. Magnified is the cell membrane, together with filaments of the cytoskeleton, and some different types of membrane-residing proteins, so called membrane proteins.*

amphiphilic molecules are parameters that determine how they assemble[36].

The cell membrane contains many different lipid species, that are generally divided into three major groups: *phosphoglycerides*, *sphingolipids* and *sterols*. In addition to the diversity in lipid composition the cell membrane also contains a multitude of proteins with a variety of purposes. Membrane-spanning proteins are for example responsible for transport of specific molecules across the membrane as well as for detection and transduction of chemical signals into the cell from the outer environment. However, the cell membrane is far from a static non-flexible biological entity. In 1972, Singer and Nicolson proposed that the cell membrane could be described as a two-dimensional fluid of oriented lipids and proteins[37]. This so called *fluid mosaic model* has had a great influence on the understanding of membrane function and topology. However, in 1982, Karnovsky et al. demonstrated that the movement of some membrane proteins was constrained, most likely due to interactions with cytoskeletal components. They also showed heterogeneity in the lateral distribution of lipids and argued that this might be of functional as well as structural significance, leading the way for the concept of *lipid rafts*[38].

The plasma membrane with its numerous constituents and intricate molecular interplay is a true marvel created by nature itself, and in addition to lipids, it hosts many different proteins with essential functions. Thus, gaining a better understanding of the plasma membrane is as important as cumbersome.

2.3 G protein-coupled receptors

G protein-coupled receptors, or GPCRs, are the largest and most diverse family of cell-surface receptors in eukaryotes. Their function is to mediate a wide variety of signals into the cell from the external world as well as from other cells in the body. To accomplish this function the receptors, embedded in the plasma membrane, each have an extracellular part able to specifically recognize individual molecules. Upon binding of a molecule to such an extracellular part of a matching receptor, a signal is transferred downstream in the cell via reactions involving proteins, nucleotides and metal ions. Finally, this chain of reactions leads to a physiological response of the cell, a response that will occur without the receptor-binding molecule having physically passed across the cell membrane. Our sight, taste and smell are examples of systems that depend on recognition and signal transfer involving GPCRs. The diverse functions of this class of membrane proteins is manifested by their ability to specifically detect various molecules such as peptides, hormones, lipids, neurotransmitters, ions, odourants, tastants and even photons[39].

Despite the variety in function and molecules they are capable of specifically recognize, all GPCRs share some common features. The single polypeptide chain, building up the protein, forms a globular structure that passes through the plasma membrane *seven* times, which explains the alternative name *seven-transmembrane (7TM) receptors*. Also, most GPCRs relay signals intracellularly via water-soluble G proteins, as the name implies. However, there are examples where the signal is transferred via other proteins, which makes 7TM a more appropriate name for this family of receptors.

Due to their diversity and the important functions they are responsible for, this class of receptors is a main target for pharmaceuticals. It is estimated that around 50% of all marketed drugs target GPCRs or the signal pathways they are involved in[40]. This emphasizes that a better understanding of this class of receptors along with an extended toolbox for studying them is of great importance for modern medicine and future drug development. Furthermore, arguing for the significance of GPCRs it is inevitable not to mention the 2012 Nobel Prize in Chemistry, which was jointly awarded to R. Lefkowitz[41] and B. Kobilka[42;43] *"for studies of G-protein-coupled receptors"*. As a matter of fact, the Nobel Prize in Physiology or Medicine 1967, 1971, 1988, 1994 and 2004 have all been related to GPCRs. The interested reader is referred to the excellent *Scientific Background on the Nobel Prize in Chemistry 2012* by Sara Snogerup Linse in the Royal Swedish Academy of Sciences reviewing the biological function and importance of GPCRs[39].

The intention of the work in **papers I** and **II** has been to develop complimentary methods for investigating GPCRs and molecular interactions involving this class of receptors. GPCRs are generally very sensitive and preserving their natural environment is a key factor to maintain their function[3]. Furthermore, the low natural abundance of GPCRs in the cell membrane forces most techniques to rely on protein enrichment via e.g. genetic overexpression[44] or detergent solubilization and reconstitution[45]. Here, we have made an attempt to develop methodologies that circumvent these challenging preparative steps

with the ultimate aim being to enable measurements that are compatible with endogenous expression levels and that still correspond well with the natural responses of this kind of receptors.

2.4 Phospholipases

Lipases are a group of enzymes that catalyze the hydrolysis, i.e. breaking down, of lipids (fat molecules) and have essential roles in many different biological processes[46]. The dietary system for digestion, transport and processing of lipids from food, cell signaling, and inflammation are just a few examples. The hydrolytic action of lipases on lipids in practise means that specific bonds in the glycerol backbone (of the lipids) are disrupted by the addition of a water molecule, and in this way e.g. a fatty acid tail can be separated from the lipid headgroup. Interestingly, lipases are also used in e.g. making of cheese and yoghurt, as well as for industrial applications in laundry detergents and production of biofuels[46;47].

Phospholipases are a subgroup of lipases that exert their hydrolytic action on phospholipids. In **paper III** a new method for detecting phospholipase A2 (PLA2) was developed. PLA2 is an enzyme that cleaves the bond by the second carbon of glycerol backbone of the phospholipid, illustrated in figure 2.3, which leads to separation of one of the fatty acid tails from the lipid headgroup. Several pathological diseases, such as cancer[11;12], acute pancreatitis[13], coronary heart dieseases[14] and ischemic stroke[14], are known to influence the concentration and/or enzymatic activity of PLA2 which makes PLA2 an interesting biomarker for diagnostic purposes as well as a target for drug development.

2.5 MicroRNA

MicroRNA (miRNA), first discovered in early 1990's[48], are short sequences (between 17-25 nucleotides) of non-coding RNA that are involved in regulating gene expression in cells. The regulation of the gene expression is achieved by the miRNA (after forming a complex with argonaute proteins) binding to the messenger RNA (mRNA) and in this way block translation at the ribosomes. Additionally, the miRNA-protein complex increases the rate at which the mRNA degrades, which also slow down the rate of translation.

The significance of miRNAs as regulators of gene expression is obvious from the fact that approximately 30% of the protein-coding genome is estimated to be regulated by miRNAs[49] and over 1900 miRNAs have been found that have important regulatory functions, involving most physiological processes[50]. In light of this, several studies have shown that altered expression levels of miRNAs may have a significant impact on health, which thus makes miRNAs suitable biomarkers. Further, altered expression levels of miRNA can for

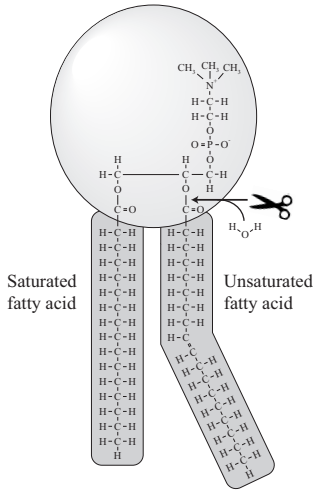

Figure 2.3: *A schematic illustration of the hydrolytic action of phospholipase A2 on a phospholipid (here POPC). The enzyme specifically targets and hydrolyze the acyl bond by the second carbon of the glycerol backbone, by addition of a water molecule, making the unsaturated fatty acid release from the lipid headgroup.*

example be associated with viral infection where miRNA can regulate and control viral replication[51].

In **paper IV** an assay was developed for highly selective detection of a certain miRNA (miR-29a), which is a clinically relevant biomarker for influenza virus infection[15].

2.6 Viruses

Viruses are small (20 nm - 400 nm) agents capable of infecting all cellular life. Each virus particle holds genetic material, in the form of RNA or DNA, surrounded by a protein capsid. Some virus particles have an additional lipid envelope enclosing the protein capsid. Since viruses can not reproduce themselves they need to take advantage of other cells, in a parasitic way, in order to survive. By attaching to the membrane of a host cell, the viruses can subsequently make their way into the cell and hijack the cellular replication machinery. In this way, new virus particles are generated, that in turn can affect new host cells. Despite the negative associations the general public might have towards viruses, they have actually contributed to develop higher forms of life through infections and transfer of genetic material. It is in fact estimated that around 8% of our genome is of viral origin[52].

The life cycle of a virus particle is usually divided in separate processes, each very complex in itself, such as attachment to the membrane of the host cell, translocation across the cell membrane[53], replication of the genetic material[54] as well as escape from the host cell[55]. However, this thesis mainly focuses on virus particles binding to gangliosides and

membrane proteins, and exploit this for the purpose of detection (**paper V**) or deduce a specific pathway for viral entry to a certain host cell (**paper II**).

In **paper II** a surface-based platform was developed to verify the physical interaction between the human cytomegalovirus (HCMV) and a specific GPCR. In **paper V** a solution-based assay for simple and rapid virus particle detection was developed. Detected were virus-like particles (viruses particles where the genetic material inside the protein capsid has been removed) of the Simian virus 40 (SV40).

3

Biomolecular sensing

In its broadest definition, a biosensor is an analytical device that either *contains* and/or *responds to* the interaction with a biological element. Arguably, a more modern definition would be restricted to the requirement of the device *containing* a biological element [56;57]. All biosensors consist of an element for recognizing the target of interest (referred to as the analyte) along with a transduction mechanism that converts the sought recognition of the analyte into a signal that is more easily detected and measured. The transduction mechanism can be optical, electrochemical, thermal, magnetic, mechanical, piezoelectric, etc. A reader device is used to process the transduced signal and present the information to the user in a comprehensible way. Preferably, the detected signal is proportional to the amount of target analyte that is detected [58].

Even though biosensors may have vastly different designs and application areas there are some aspects that defines a well-functioning biosensor. The first critical aspect is a high *selectivity* for the target analyte, which means that the recognition element interacts favorably only with the target analyte (even in a crowded environment). Also, it is important that the target analyte interacts *specifically* with the recognition element, and thus not *unspecifically* with other parts of the sensor that might yield a signal [†]. Other important aspects are the ability to generate essentially identical responses once repeatedly exposed to the same sensing conditions, i.e. high level of *reproducibility*. Additionally, the biosensing setup should be *stable* against external disturbances. All these aspects contribute to the overall *robustness* of the biosensor, which combined with ease of use, sensitivity, fast response time and low price are desirable properties of modern biosensors.

3.1 Perspectives on biosensing

From a historical perspective, one of the earliest examples of biosensing is the use of caged-in canary birds for detecting toxic gases in coal mines. In the 1890's John Scott Haldane,

[†]Other definitions of *selectivity* and *specificity* might appear in the literature, but throughout this thesis the definitions given above will be used.

a Scottish physiologist, introduced the use of canaries in coal mines as an early warning system for build-up of for example carbon monoxide and methane, and other toxic gases. Canaries, and birds in general, are very sensitive to toxic components in the air because of their breathing anatomy and comparably fast rhythm of breathing. Thus, once the caged birds stopped singing and fell down dead the miners knew it was time to evacuate the shaft. Even though the canaries were replaced by electronic gas detectors already before the 1900's several modern biosensing techniques take advantage of living microorganisms to detect toxic or other harmful substances. Speaking examples, because of their names, are the CANARY (cellular analysis and notification of antigen risks and yields) technology developed at MIT's Lincoln Laboratory, where genetically engineered B cells are used to detect and identify airborne pathogens[59], and the nanocanary technique developed at University of Massachusetts Lowell, where macrophages are used to assess the toxicity of engineered nanomaterials such as carbon nanotubes[60]. Even though Haldane's caged canaries might have saved many lives he was never formally recognized for inventing the first biosensor. Instead, Leland C. Clark Jr., an American biochemist, was honored as the "Father of Biosensors" at the 1992 World Congress on Biosensors in Geneva, Switzerland, for his invention of the Clark electrode in 1956; a device for measuring oxygen levels in blood, water and other liquids[61].

Despite the many application areas for biosensors, there are relatively few commercially available biosensor for personal use. One of the most wide spread biosensor is the glucose meter widely used in for example self-management of diabetes. In 1963, the first step towards today's glucose meter was taken by Ernie Adams, upon developing a paper strip that turned blue when exposed to glucose. The intensity of the blue color was proportional to the glucose concentration, which implied that the actual glucose level had to be determined by comparison with a calibration chart. Today, glucose meters come in different designs. The traditional approach is to have an enzyme (glucose oxidase, glucose dehydrogenase, or hexokinase) react with the glucose in the blood. Measuring the presence of generated products, for example hydrogen peroxide, via interaction with a dye is one of several ways to give the user an approximate value of the glucose levels in the blood (typically in the mM range) within seconds[62]. However, most modern glucose meters are based on an electrochemical readout[63].

Another example of a commercially available biosensor that have greatly impacted our society is the pregnancy test. Originally developed in the 1970's the test is used to detect human chorionic gonadotropin (hCG), a hormone produced by the placenta after the fertilized egg has adhered to the uterus and thus a suitable biomarker for pregnancy[64]. The test is available in more than 10 different variants, but a common one is the strip test that consists of a capillary membrane used to transport the analyte over different zones on the strip. First, the urinal sample passes over a reaction zone of the strip. Here, monoclonal anti-hCG antibodies conjugated to enzymes reside. If hCG is present in the urinal sample they can bind to the these antibody-enzyme complexes, now dissolved and part of the capillary flow. Next comes the test zone, where polyclonal anti-hCG and inactive dye is immobilized on the surface. In case of pregnancy, the formed complexes of hCG and

monoclonal anti-hCG (carrying an enzyme) now bind to immobilized antibodies, which allows the antibody-conjugated enzyme to activate the dye, which makes the test region light up and become visibly colored.

With the glucose meter and the pregnancy test being two prominent biosensors for commercial use at home some interesting aspects can be noted. Both of these biosensors have a sensitivity in the right concentration range for the analyte to be detected (μM - mM) accompanied by robustness and a fairly good precision making the sensors reliable. This in combination with the comparably low cost and the ease of use are all key factors for a successful biosensor for commercial use. Even though other commercial well-established biosensors or sensing protocols, such as for example the enzyme-linked immunosorbent assay (ELISA)[16], or the polymerase chain reaction (PCR)[65], are capable of detecting and quantifying other types of biomarkers with higher sensitivity for diagnostic purposes, they generally require labor intensive sample preparation, expensive detection schemes, and/or complicated analysis. One aim of this thesis work has been to explore concepts that might open up for simple yet sensitive biosensors.

3.2 Biosensing formats

The importance of biosensors in our modern society was foreseen already in the influential interdisciplinary work by Turner et al. from 1987[58]. The authors predicted that the powerful combination of the specificity offered by biological components and the microelectronic components together with strong computational power held great potential for future biosensing. In addition to applications in diagnostics and drug discovery, biosensors can also be used to monitor personal health and fitness, quality of food, as well as the external environment[66], to mention some areas of use.

Arguably already fulfilled, the prophecy of Turner et al. required the versatility of biosensors in combination with clever sensing formats and readout schemes to be exploited. As was mentioned earlier, a biosensor consists of a recognition element, which could be receptors, enzymes, antibodies, nucleic acids, etc.[67] This in combination with different transducer mechanisms (optical, electrochemical, thermal, magnetic, mechanical, piezoelectric, etc.), and many different readout principles offer a plethora of biosensing schemes, together covering a wide range application areas.

To give a better overview of the different types of biosensing schemes they are often categorized. One such categorization relates to the type of biorecognition element that is used. Catalytic-based sensors utilize the action of enzymes to detect the analyte (substrate to the enzyme); for example the glucose sensor. Affinity-based sensors instead utilize the physical binding of the analyte to the recognition element to induce a detectable signal; for example the pregnancy test. Further, the sensing schemes can be categorized based in how the signal readout is performed. There are time-resolved measurements and end-point

measurements. Here, the former allows for information about the interaction kinetics to be resolved as the binding and release processes can be readily followed. Also, depending on if the sensing schemes require labeling of one of the interacting biomolecules (for example fluorescent or radioactive molecules) they are classified as either label-free or not.

In this thesis different biosensing schemes have been developed both for studying biomolecular interactions and detection of biomarkers and pathogens. In terms of biosensing formats **papers I** and **II** are surface-based; having one of the interacting partners immobilized on a surface. Surface-based assays have the benefit of offering the possibility to inject multiple solutions over the same surface, and often each injection step can be monitored separately (in time-resolved measurements) for easy and reliable readout, which also offers simplified troubleshooting. However, the objective of the thesis transitioned for the second part (**papers III**, **IV**, and **V**) into developing solution- rather than surface-based assays. The solution-based assays arguably are more similar to the situation occurring *in vivo* as none of the interact partners necessarily needs to be immobilized on a surface, an action that can potentially alter the interaction characteristics of the biomolecule. Additionally, the interaction kinetics are faster which allows for more sensitive detection. Yet another important aspect is the ability to design biosensing schemes that contain few experimental steps, and possibly be as easy as mix-and-measure. Incorporated together with cheap detection systems such sensors might increase their availability for example in facilities with scarce resources.

As is evident from above different sensing formats have different advantages, and care needs to be taken to choose biosensing assay based on the purpose of the measurement, such that for example i) the sensitivity range covers the expected concentration span of the analyte, ii) the sensor is compatible with the complexity of the sample, and iii) the readout provides the information sought. Despite the lack of a generic sensor for all purposes some methods have become more well-established than others. The enzyme-linked immunosorbent assay (ELISA), developed in the 1960's, and the polymerase chain reaction (PCR), developed in the 1980's, are two prominent examples nowadays being standard methods in clinical diagnostics and research laboratories.

Despite many well-performing biosensing assays there are still major challenges that remain to be resolved. Assays for simultaneous detection (and concentration determination) of several analyte molecules in a single sample, so-called multiplexed assays, is an important step for improved diagnostics, since for example the same biomarker might have altered expression levels for several disease states. Additionally, detection of clinically relevant biomarkers present at extremely low concentration (typically < 1 aM, corresponding to less than ~ 600 molecules per ml), in a reliable way remains very challenging. In light of the latter challenge, there have been many reports on the development of methods with extra-ordinary sensitivities. However, the transition of such findings to commercial diagnostic assays are surprisingly rare.

3.3 Single-molecule sensitivity

Even though traditional bioanalytical sensing relies on measuring the response from the collective ensemble major activities have been spent on developing methods to circumvent this. By improved instrumentation for detection new bioanalytical sensing schemes have emerged with the ability to resolve individual interactions, at the so-called single-molecule level, which represents the ultimate resolution limit. By being able to decompose an ensemble signal into the contributions from individual interactions, it is possible to unravel heterogeneities with respect to the biomolecular interactions. Additionally, the single-molecule detection level possibly offers a more competitive sensitivity than the ensemble-averaging counterpart. Two examples of biosensors that can provide detection at the level of single molecules (even label-free) are sensors based on the so-called whispering-gallery-mode[68] and single-molecule ELISA termed SiMoA (single-molecule arrays)[69].

All bioanalytical assays developed in this thesis have been realized in a manner that allows for single-molecule readout. In the surface-based assays presented in **papers I** and **II** the ability to resolve single interactions was readily used to effectively sort out unspecific interactions with the underlying substrate and also to be able to measure interaction kinetics at equilibrium, i.e. without advanced liquid handling schemes. In the solution-based assays for biomarker detection presented in **papers III** and **IV** the single-molecule resolution did not offer a much improved limit-of-detection *per se*, but aided in gaining a deeper understanding for the courses of events that lead to the measured signal. In **paper V** the ability to image individual nanoparticles was a prerequisite to detect an early onset of an aggregation process, induced by the presence of a pathogen, which would have been very difficult, if not impossible, to realize in a setup measuring the aggregation state of the ensemble in for example turbidity measurements. In the outlook section (6.2) suggestions on how the limit of detection might be even further improved are included.

4

Experimental methods and concepts

The fundamental steps necessary in the development of experimental assays for studying biomolecular interactions usually involves biological model systems of different levels of complexity. Additionally, several different instruments and techniques originating from various scientific disciplines are often used along the way. This chapter gives a brief overview and explanation of the four major techniques playing a key role in the projects presented in this thesis. Additionally, the concept of fluorescence and Förster resonance energy transfer (FRET), and their role in biological research is briefly discussed.

4.1 Quartz crystal microbalance with dissipation monitoring - QCM-D

QCM-D is an acoustic label-free high-sensitivity technique widely used for biosensing applications[70;71]. The technique is capable of measuring the mass adsorbed to the sensor surface allowing for studies of for example protein interactions[72], biopolymers[73] and even cells[74;75]. The mass adsorbed on the sensor surface can be measured with a sensitivity of down to 1 ng/cm^2 and the technique can be applied to biological and chemical entities ranging in weight from less than 200 Da up to several GDa[76]. From the dissipation measurements, structural parameters like elasticity and viscosity of the system can be modeled.

The sensing method is based on the piezoelectric property of crystalline quartz, a phenomenon thoroughly investigated in 1880 by Jacques and Pierre Curie[77]. Crystalline quartz consists of a continuous framework of tetrahedral SiO_4-units ordered in a trigonal crystal system. The chemical formula, SiO_2, is a consequence of each oxygen being shared between two tetrahedra. Physical deformation of the crystal induces dipole moments, which in turn generate electrical charges on the crystal surface. Similarly, exposure to an electric field induces a physical deformation of the crystal, a phenomenon named *the converse piezoelectric effect*. By applying an alternating electrical potential across an AT-cut

quartz crystal, 35.25^o to its optical axis, a thickness-shear mode oscillation is induced. An acoustic wave is created in the crystal, propagating in the direction perpendicular to the surface[78], and the frequency at which half of its wavelength exactly matches the crystal thickness is called the *resonance frequency*[70], f_n. Similarly, the resonance condition is fulfilled if an odd number of half wavelengths match the crystal thickness. At resonance the crystal oscillation amplitude reaches a maximum and the energy losses are minimal. The resonance frequency is determined as

$$f_n = \frac{nv_q}{2t_q} = \frac{nv_q}{\lambda} \tag{4.1}$$

where n is the number of the odd harmonic, t_q is the thickness of the quartz crystal, v_q is the speed of sound in quartz (3340 m/s perpendicular to the sensing surface) and λ is the wavelength of the acoustic wave. Figure 4.1 shows a schematic illustration of the setup and how the quartz crystal oscillates along with a photography of a QCM-D instrument.

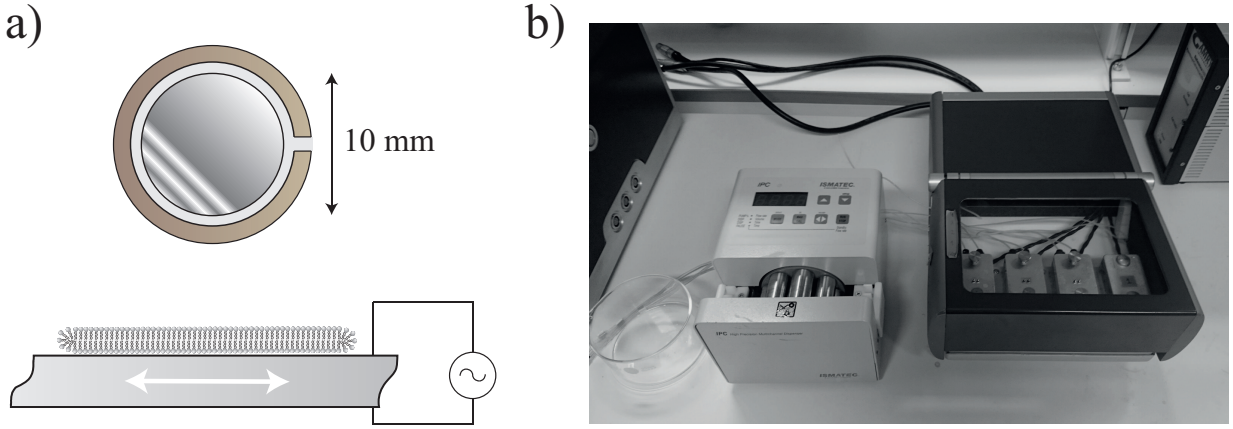

Figure 4.1: ***a***) *A schematic illustration of a quartz crystal as a sensing device (top view and side view with an SLB. An alternating electrical potential makes the crystal oscillate in a thickness-shear mode as the white double arrow indicates. When an odd multiple of* $\lambda/2$ *of the acoustic wave created matches the thickness of the crystal the resonance condition is fulfilled.* ***b***) *A photography of a QCM-D E4 instrument where four different sensor surfaces can be monitored simultaneously. To the left is a peristaltic pump.*

The *Sauerbrey relation*[79], equation (4.2), which states that there is a linear relationship between adsorbed mass and shift in resonance frequency of the crystal, is one of the key bridges between measurements and results.

$$\Delta m = -\frac{C\Delta f}{n} \tag{4.2}$$

Where Δm is the change in adsorbed mass per area unit and Δf is the change in resonance frequency. The mass sensitivity constant C equals 17.7 ng/(Hz cm^2) for a 5 MHz crystal

and n is the number of the odd harmonic used. The relation holds for rigid, evenly distributed and sufficiently thin adsorbed layers of molecules. When an adsorbed layer does not fulfill these requirements the Sauerbrey relation underestimates the mass of the layer. By combining information on shifts in resonance frequency and dissipation from multiple harmonics with viscoelastic models, the thickness, shear elastic modulus, and viscosity of the adsorbed molecular layer can be estimated [80]. This contributes to the characterization of the adsorbed layer even though it is out of the Sauerbrey regime. Figure 4.2 shows the result of a typical experiment that can be performed in a QCM-D instrument. A bilayer formation is presented along with an illustration of corresponding liposome adsorption and rupture. A well-formed bilayer is typically characterized by a Δf around -27 Hz and a ΔD close to zero [81].

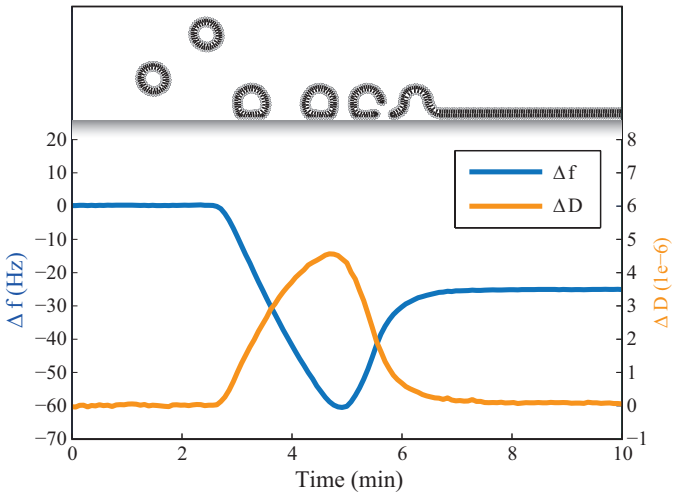

Figure 4.2: *A QCM-D graph showing the formation of a supported lipid bilayer. The blue curve represents the resonance frequency shift (Δf) for the fifth harmonic. The orange curve represents the dissipation shift (ΔD). The illustration above the curve is in accordance with the time axis and shows how liposomes adsorb on the surface and rupture into a bilayer when a critical coverage is reached. During the liposome rupture the buffer inside the liposomes de-couples from the sensor surface and the lipids form a more rigid structure. This is seen as an increment in Δf and a decrement in ΔD.*

The QCM-D technique was used in **paper I** for evaluating different coupling chemistries for immobilization of chemokine ligands on a supported lipid bilayer. Furthermore, it was used to confirm specific binding of GPCRs contained in native membrane vesicles to the immobilized ligands. The surface chemistry could then be transferred to the total internal reflection fluorescence (TIRF) microscope, where ligand-receptor interactions could be studied at a single-molecule level.

In a similar way QCM-D was used in **paper V** to verify that liposomes with incorporated gangliosides (GM1) bind to SV40 VLPs, and can thus potentially be used as reporters for detecting the presence of SV40 VLPs in solution.

4.2 Fluorescence and spectrofluorometry

4.2.1 Fluorescence

One central and often employed concept in studying biological structures and processes is fluorescence. The phenomenon comprises that certain molecules, atoms or nanostructures upon absorption of light immediately emit light of longer wavelength (lower energy) than they absorbed [82]. Briefly, the underlying physical principle is that the substance (here termed fluorophore) has a certain energy gap in the range of the photon energy corresponding to visible light (IR and UV are also possible). Upon absorption of an incoming photon an orbital electron is brought from the ground state (S_0) to the first excited singlet state (S_1). This excited state is not a stable state and relaxation down to the ground state occurs through both radiative and non-radiative pathways, each with a different probability. The radiative process where the electron jumps from S_1 to S_0 by emitting a photon of corresponding energy is termed fluorescence, as is illustrated in figure 4.3a.

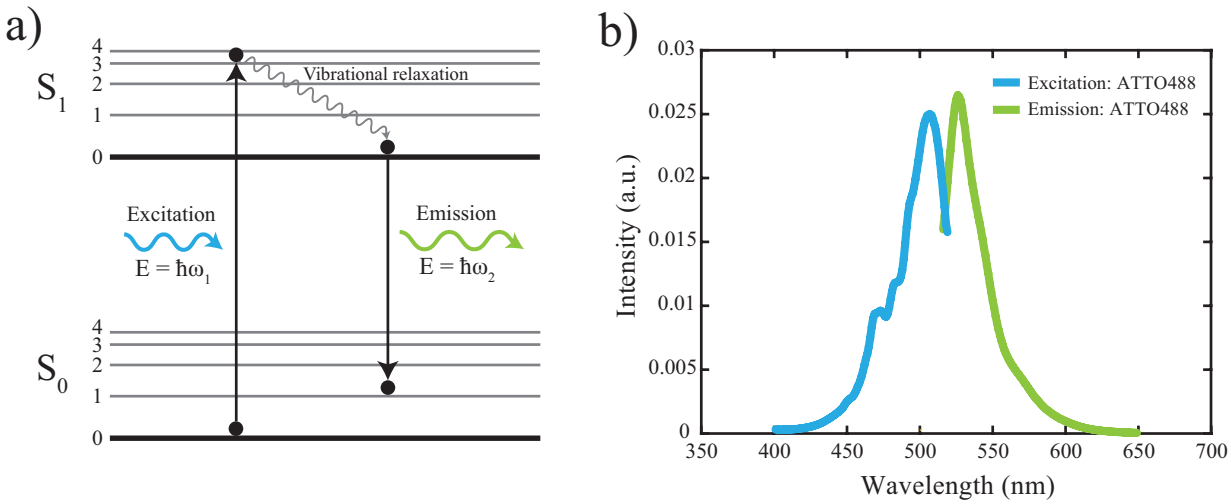

Figure 4.3: ***a***) *A Jablonski diagram illustrating the concept of fluorescence. A high energy photon (blue) transfers its energy to an electron of a fluorophore and brings it from the ground state (S_0) to the first excited single state (S_1). After rapid relaxation to the lowest vibrational level of S_1 the electron jumps down to the ground state by emitting a photon of corresponding energy (green). Note that the energy of the emitted photon is lower than the absorbed ($\omega_1 > \omega_2$), and hence its wavelength is longer.* ***b***) *Example of an excitation and emission spectra for a fluorophore (here ATTO488). The discrepancy in wavelength between the excitation and emission light, i.e. the Stokes shift, is utilized in for example fluorescence microscopy to distinguish the light emitted by the fluorophores from background illumination and scattering.*

As previously mentioned, taking advantage of fluorescence is common in biological research to image small scale objects and processes, that alone do not interact sufficiently with light

to be visualized with a regular light microscope. Fluorescence labeling of these "invisible" objects increases their interaction with light which makes them visible in a fluorescence microscope. As depicted in figure 4.3b there is a significant discrepancy in the wavelength between the absorbed and emitted light of fluorophores (called the *Stokes shift*). A fluorescence microscope takes advantage of this and uses filters to monitor only light with longer wavelength than the excitation light for creating the image to effectively suppress the background and sort out only the light originating from fluorescence.

Fluorescence has been a central concept in all five papers appended in this thesis to enable visualization of biomolecular interactions (**papers I** and **II**), but also for reporting the presence of biomarkers or virus particles in solution (**papers III**, **IV** and **V**).

4.2.2 Förster resonance energy transfer (FRET)

Fluorescence is a very versatile phenomenon that can be exploited in many different ways. One process that has been employed in both **papers I**, **III** and **IV** is that of Förster resonance energy transfer (FRET). This is a process of energy transfer, illustrated in figure 4.4, from a fluorophore (donor) having an emission spectrum overlapping with the excitation spectrum of another fluorophore (acceptor). The energy transfer occurs through a dipole-dipole interaction and is thus a non-radiative process.

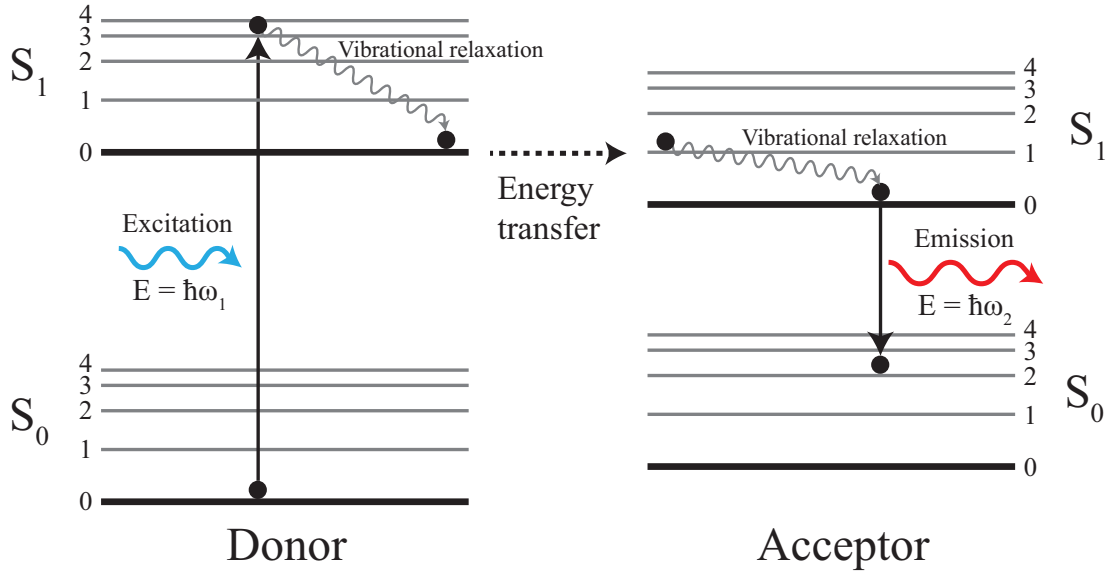

Figure 4.4: *Jablonski diagram illustrating Förster resonance energy transfer (FRET). An excited fluorophore (donor) transfers energy to another fluorophore (acceptor) through a non-radiative process (dipole-dipole interaction). When the acceptor fluorophore jumps back to the ground state a photon is emitted with significantly lower energy than the photon first absorbed by the donor ($\omega_1 > \omega_2$).*

The rate of energy transfer from donor to acceptor separated by a distance r is given by[82;83]

$$k_T(r) = \frac{Q_D \kappa^2}{\tau_D r^6} \left(\frac{9000(ln10)}{128\pi^5 N n^4} \right) J(\lambda) \tag{4.3}$$

where Q_D is the quantum yield (number of emitted photons relative to the number of absorbed photons) of the donor (in absence of acceptor), κ^2 describes to the relative orientation between the transition dipoles of the donor and acceptor (equal to 2/3 for random averaging), τ_D is the lifetime of the donor (in absence of acceptor), N is Avogadro's number, n is the refractive index of the medium, and $J(\lambda)$ describes the spectral overlap between the donor emission with the acceptor excitation.

To get a better feeling for what this rate of energy transfer implies it is usually rewritten in terms of a so-called *Förster distance* (R_0). At this distance half of the excited donor fluorophores decay through energy transfer, and half through the usual decay paths in absence of the acceptor, i.e. at the Förster distance $k_T = \tau_D^{-1}$. The Förster distance is typically in the range of 1.5 to 6 nm[82]. As is evident from equation (4.3) the FRET efficiency is strongly dependent on the distance r between donor and acceptor fluorophore (r^{-6}). As a reference the FRET efficiency drops from 98.5% to 1.5% in the distance interval $0.5R_0$ to $2R_0$. This in combination with the short Förster distance makes FRET an efficient means to probe inter- and intramolecular distances in the nanometer range. FRET has been employed in a multitude of ways to for example detect molecular interactions[84], assess protein folding[85] or monitor lipid exchange or mixing and membrane fusion[86–88]. Note that FRET can be detected as a decrease in donor emission or as an increase in acceptor emission.

In this thesis FRET was used to verify lipid mixing and liposome fusion. In **paper I** a FRET assay (between NBD and Rhodamine) was used to confirm that native membrane vesicles (from a certain cell line) could be fluorescently labeled by sonicating them together with fluorescently labeled (synthetical) liposomes, a protocol adapted from[89;90]. In **paper III** FRET (between ATTO488 and ATTO633) was used to detect lipid rearrangements in a solution of liposomes (for example micelle formation, lipid mixing, and liposome fusion) subjected to the hydrolytic action of PLA2. In **paper IV** FRET (between DiI and DID) was used to detect DNA-mediated fusion between liposomes.

4.2.3 Spectrofluorometry

Spectrofluorometry is a versatile technique used to study spectral properties of various fluorescently labeled samples. One common setup, depicted in figure 4.5, is based on having a high intensity light source with a broad spectrum from IR to UV (white light). The light from the light source first goes through an excitation monochromator, where it is decomposed in different wavelength by reflection on a diffraction grating. The wavelength

of the light exiting the monochromator (through a narrow slit) can be controlled by rotation of the grating. The light, used for excitation, is then focused onto the sample and readout is then carried out at a specific angle to the excitation (in our case at 90^o). The emitted light then passes through a monochromator, adding the possibility to decompose the different wavelengths, before hitting a photomultiplier tube (PMT). The PMT converts the photons to an electrical signal that is monitored by a computer.

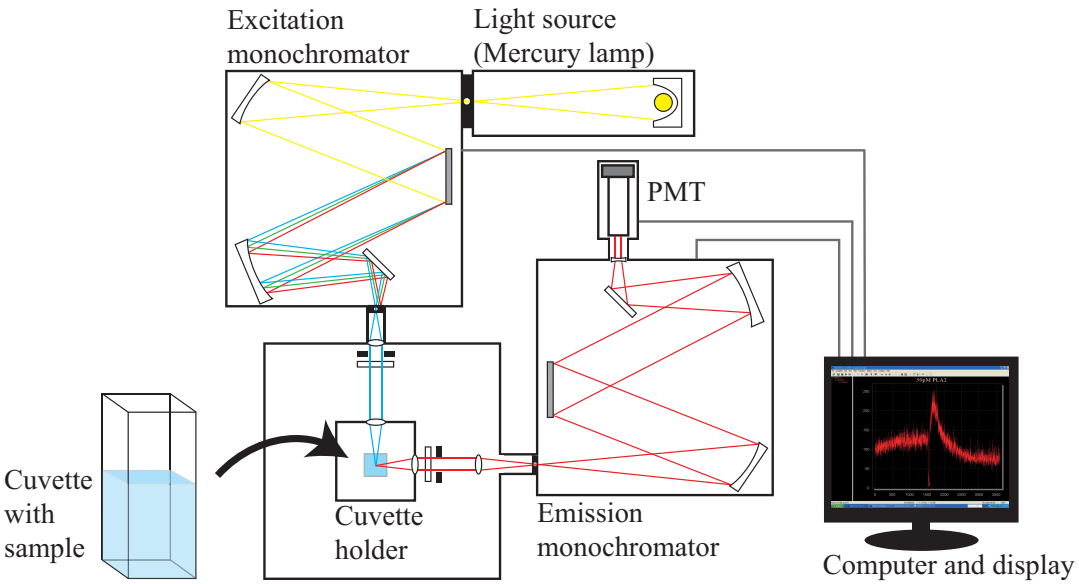

Figure 4.5: *Illustration of a spectrofluorometer. A mercury lamp delivers white light that is passed through an excitation monochromator to enable any wavelength in the range to be used for sample excitation (here blue). The light emitted from the sample (red), perpendicular to the excitation light, is passed through a second monochromator before being quantified by a photomultiplier tube (PMT) connected to a computer.*

Spectrofluorometry was in this thesis mainly used to study samples of suspended liposomes. In **paper I** the decrease in FRET signal was monitored for a NBD-Rhodamine pair to verify that lipids from synthetical liposomes were mixed in native membrane vesicles upon sonication. In **paper III** the emergence of FRET between the ATTO488-ATTO633 pair was monitored to study lipid rearrangements among synthetic liposomes subjected to the hydrolytic effect of PLA2. In **paper IV** a microplate-reader system, with essentially the same components as the spectrofluorometer descibed above, was used to detect liposome fusion via an increased FRET ratio (acceptor emission/donor emission). The FRET pair used was the lipophilic dyes DiI and DiD [91].

4.3 Total internal reflection fluorescence microscopy - TIRFM

The key concept for studying the individual molecular interactions, in the surface-based assays developed in **papers I** and **II**, was to exploit a very sensitive readout principle. Fluorescence microscopy is a versatile technique that, in combination with keeping the transmembrane proteins in a vesicle format, can be used to visualize the ligand-receptor interaction without directly labeling either of the two interacting entities [92]. However, in a standard fluorescence microscope not only the fluorescent molecules attached to or in close proximity of the surface are visualized, but also those present in the relatively deep focus volume. This results in a substantial background signal that makes it difficult, if not impossible, to distinguish individual binding events on the surface. Upon total internal reflection of the excitation light at the substrate-liquid interface, an evanescent wave is created. This wave propagates parallel to the substrate and penetrates approximately one light wavelength into the liquid medium. This evanescent field is capable of exciting fluorophores, but it decays exponentially, according to equation (4.5) and (4.6), which confines the excitation volume to the substrate-liquid interface. In this way the background signal is substantially reduced, which enables studies of single molecular interactions. [93]

The basic principle behind total internal reflection fluorescence (TIRF) microscopy is the refraction of light travelling between mediums of different optical densities, governed by the well-known *Snell's law*. If light travels from an optically denser to a less dense medium and the angle of incidence is increasing, a point will be reached where the refraction angle becomes 90^o. The angle of incidence at which this occurs is termed the *critical angle*, θ_c, and an expression for this angle is easily derived from Snell's law as

$$\theta_c = \arcsin\left(\frac{n_2}{n_1}\right) \tag{4.4}$$

where n_1 and n_2 denote the refractive indices of the optically denser and thinner medium, respectively. If the angle of incidence is further increased the light will be reflected instead of refracted. Even though light is not transmitted through the interface an electromagnetic field appears in the optically thinner medium, called an *evanescent field*. The intensity of the evanescent field decays exponentially with distance away from the interface according to

$$I(z) = I(0)\exp(-z/\delta) \tag{4.5}$$

where z is the distance away from the interface, $I(0)$ is the intensity at the interface and δ is the decay constant defined as

$$\delta = \frac{\lambda}{4\pi n_2}\left(\frac{\sin^2\theta}{\sin^2\theta_c} - 1\right)^{-1/2} \tag{4.6}$$

where λ is the wavelength of the light, n_2 is the refractive index of the optically thinner medium, θ is the angle of incidence and θ_c is the critical angle. A schematic illustration of a TIRF-setup along with a photography of a TIRF microscope is shown in figure 4.6.

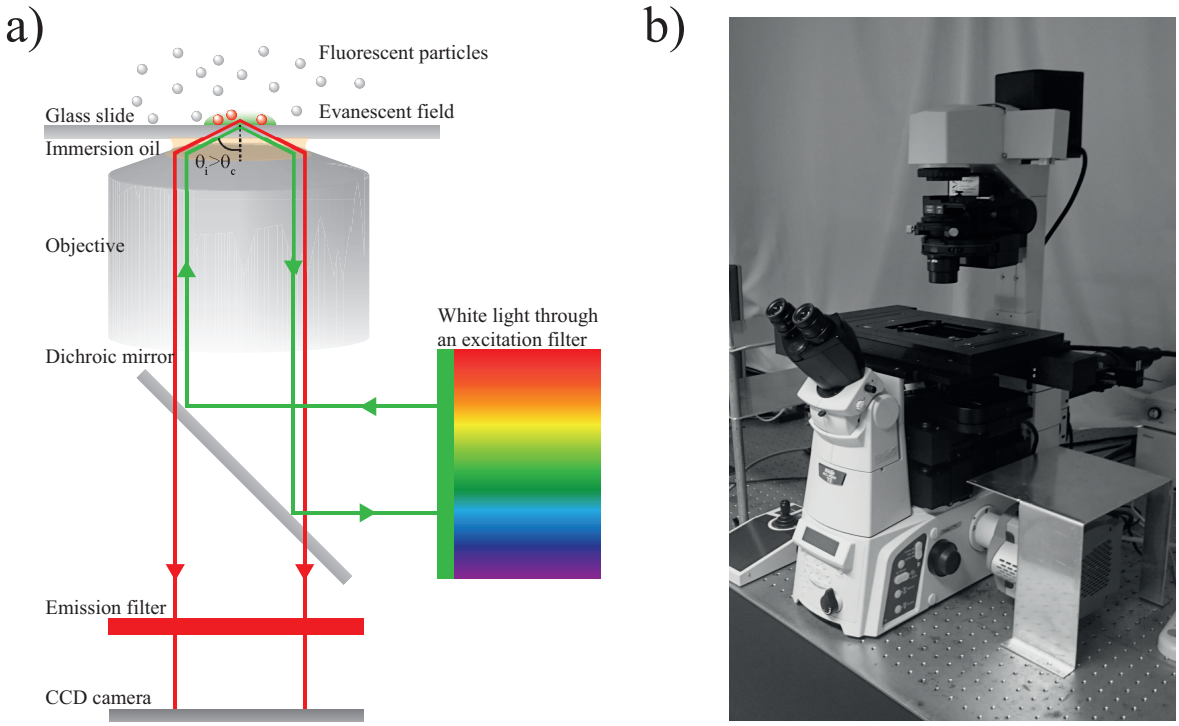

Figure 4.6: ***a***) *Schematic illustration of a TIRF-setup. White light passes through an excitation filter and monochromatic light enters the microscope. The light is directed to the objective via a dichroic mirror. A crescent-shaped aperture makes the light enter the substrate-liquid interface at an angle high enough for the beam to undergo total internal reflection. An evanescent field enters the sample volume and fluorescent molecules on or very close to the surface are excited. Subsequently, the emission light goes back through the objective and hits the detector. Selective excitation of fluorescent molecules in close proximity to the surface enables individual molecular interactions to be studied.* ***b***) *A photography of a TIRF microscope.*

In this thesis TIRF microscopy was exclusively used in **papers I** and **II** to study native membrane vesicles, proteoliposomes, or virus particles binding to surface-modified glass substrates. A representative example of a micrograph from TIRF microscopy is shown in figure 4.7. The fluorescently labeled vesicles holding membrane proteins that interact with the corresponding ligands immobilized on the surface. Single vesicles are readily

distinguished and by studying individual binding/unbinding to the surface over time information about the kinetic parameters describing the receptor-ligand interplay can be extracted.

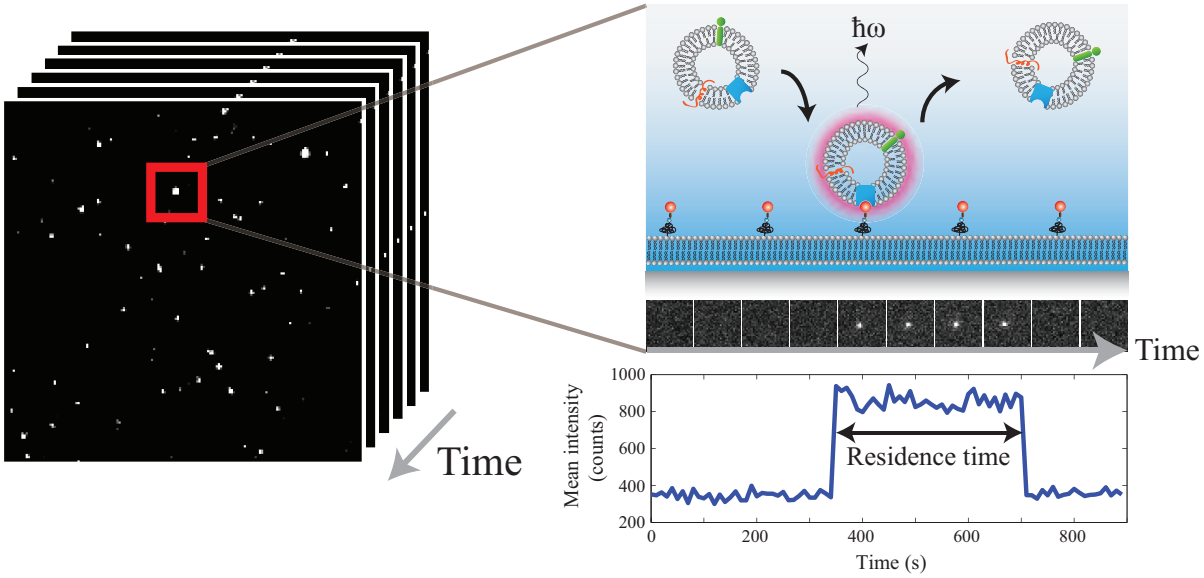

Figure 4.7: *(Left) Micrographs recorded in time-lapse mode showing individual receptor-containing vesicles attached to ligands immobilized on the substrate. (Right) A schematic showing how the residence time of single receptor-ligand interactions can be extracted from these micrographs. Through image analysis the residence times from all vesicles binding and releasing from the surface within the time-frame of the experiment are readily extracted.*

4.4 Dual-color fluorescence microscopy

Inspired by nanoparticle tracking analysis (NTA, Malvern Instruments[94]), a well-established solution-based method for nanoparticle characterization, a new technique for imaging and tracking liposomes and other nanoparticles was developed within the framework of this thesis. The technique, referred to as dual-color fluorescence microscopy, offers the possibility to image the nanoparticle sample in two different wavelength regions simultaneously. The technique is adapted to work on a standard light microscope with laser light as the illumination source. The laser light is introduced to a channel, holding the liquid sample, through an optical fiber (see figure 4.8a and b). The high intensity of the illumination enables nanoparticles to be individually imaged in both scattering and fluorescence mode.

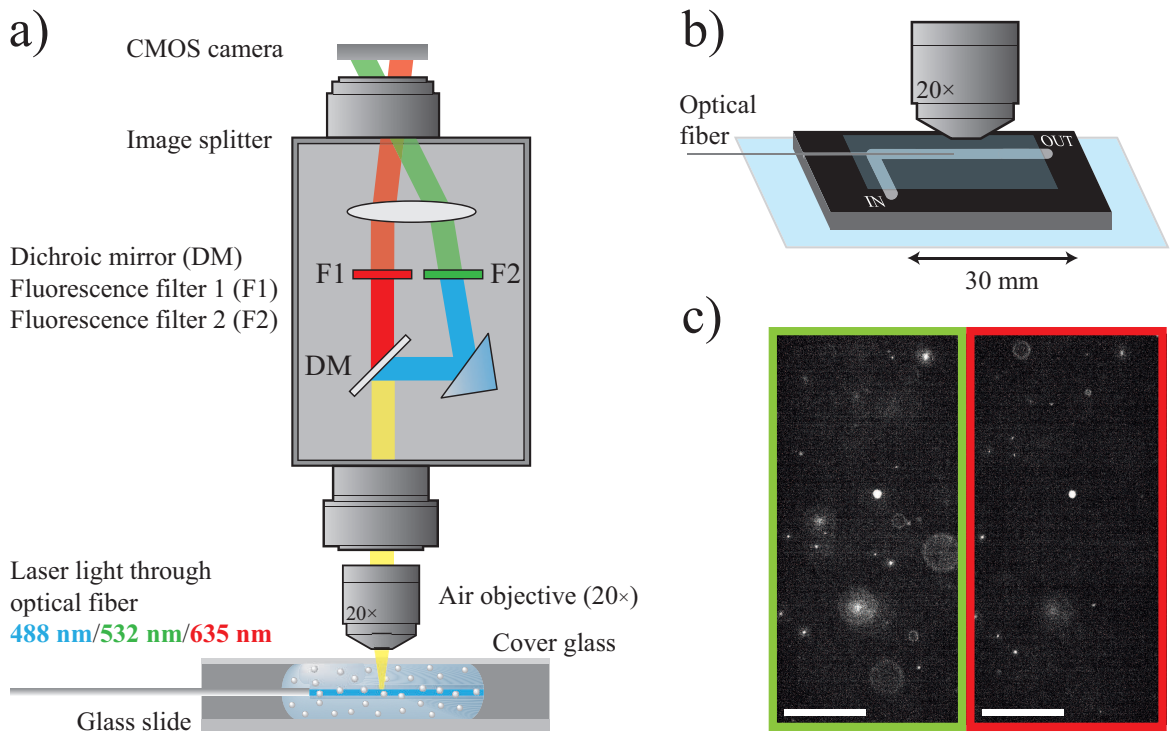

Figure 4.8: ***a***) *Schematic illustration of the dual-color fluorescence microscopy setup. Laser light coupled through an optical fiber illuminates the sample. The light emitted by the sample (either via scattering or fluorescence) passes through an image splitter before being projected onto a CMOS sensor making it possible to separate signals originating from for example different fluorophores.* ***b***) *A more detailed illustration of the sample channel molded in black-colored PDMS. A regular cover glass is used to seal the channel which also creates an inlet and an outlet, through which the channel is readily filled, evacuated, and rinsed with a regular automatic pipette.* ***c***) *Example micrographs where two different (fluorescently labeled) liposome populations (diameter* $\approx 100\,\mathrm{nm}$*) are imaged simultaneously. Here, the micrographs are taken from a colocalization experiment, which explains some overlap between the liposomes in the two channels. Scale bars are* $50\,\mu\mathrm{m}$*.*

The dual-color fluorescence microscopy setup is designed to allow for customization of illumination settings and optical components to better match the specific needs of each experiment. The illumination source can be any light source that can be readily coupled into an optical fiber. A fiber combiner can then be used to join multiple light sources allowing for multi-wavelength excitation. In the work presented in this thesis lasers of 488 nm, 532 nm and 633 nm wavelengths were used, either individually or in combination (mixed), depending on the particular experiment. In addition to wavelength alteration and mixing, the laser settings (for example intensity, exposure time, pulsing etc.) can easily be adjusted by the user for each experiment.

The image splitter, as the name implies, offers the possibility of separating a single input image into two parts based on wavelength by means of a dichroic mirror. Additionally, two fluorescence filters can be added to the setup, which enables separation of light from for example two different fluorophores or separation of fluorescent and scattered light (see figure 4.8a and c). The combination of dichroic mirror and fluorescence filters is adapted to fit the properties of the sample being studied.

The home-built sample holder, illustrated in figure 4.8b, consists of a piece of PDMS rendered non-transparent with black color to minimize the background scattering. A narrow L-shaped channel (measuring $1.5 \times 1.5 \times 40$ mm) with a total volume of ~ 100 μl was molded in the PDMS and sealed off by a thin glass slide creating an inlet and an outlet. The channel is easily filled, rinsed, and evacuated with an automatic pipette. The optical fiber guiding the excitation light is inserted into the sample chamber from the side through a small incision in the PDMS.

Being able to alter the setup with different illumination sources, filter combinations, PDMS channel dimensions, light collection optics and cameras enables the technique to be easily adapted to almost any the experimental system. This is rarely the case in similar commercially available instruments, where a certain laser source and filter set often are predefined. In addition to flexibility of illumination source and the optical components the setup also allows for custom analysis of the recorded data. The micrographs from the CMOS camera can be imported and analyzed with custom-written scripts in e.g. MATLAB (see figure 4.8c).

In this thesis the versatility of the dual-color fluorescence microscopy setup was exploited in **papers III**, **IV**, and **V**. Even though fluorescently labeled liposomes and other lipid assemblies were exclusively studied in these three papers it was of great advantage to be able to alter both the illumination wavelength and intensity, the fluorescence filters in the image splitter and customize the analysis of the recorded micrographs. To mention some examples; liposomes were counted, correlation patterns between the two fluorescence channels were studied, the overlap between the two fluorescence channels was quantified, and liposomes were tracked (in the two fluorescence channels) for liposome size determination.

5

Summary of appended papers

In this chapter a short description along with a brief summary of the main results is given for each of the five appended papers. The papers are organized in a way to illustrate how the work conducted in this thesis evolved from first relying on surface-based assays, and studies of interactions involving GPCRs, towards solution-based assays, focusing more on new concepts for detecting important disease biomarkers and virus particles in a rapid, easy and sensitive way.

To connect back to the experimental strategies when studying biological systems, briefly discussed in section 2.1, before going into each paper individually, both **papers I** and **II** take advantage of a surface to study molecular interactions with GPCRs. In both studies TIRF microscopy was used and an SLB enabled an inert surface onto which one of the interacting partners was immobilized. Further, in both studies, lipid-based vesicular structures (either as proteoliposomes or native membrane vesicles) were used to ensure that the GPCRs were kept in a near-native environment to minimize the risk of altering their function.

Although the strategies employed in the first two papers worked fairly well for studying these types of ligand-receptor interactions, we wanted explore ways of studying biomolecular interactions directly in solution instead. In this way we could avoid precarious surface cleaning protocols and possibly lower the risk of having problems with unspecific binding to the underlying substrate; issues that we invested significant efforts into solving in **papers I** and **II**. Additionally, in comparison with surface-based assays, solution-based assays can be as easy as "mix-and-measure" and thanks to diffusion and collision in three dimensions, the kinetics is faster, which possibly allows for easy, rapid and sensitive readout.

In **papers III** and **IV** we investigated two different detection methods based on biorecognition-induced lipid mixing and/or fusion (via FRET) with the biomolecular recognition and the readout occurring directly in solution. In **paper V** an alternative solution-based detection method was explored, this time with similarities to **paper II**, as colocalization of differently colored nanoparticles confirmed a specific interaction.

5.1 Paper I

In the first paper we took advantage of an already established method based on TIRF microscopy capable of extracting kinetic information of biomolecular interactions at equilibrium [92]. In many other conventional biosensing techniques, for example QCM [95] and SPR [96], the ensemble signal needs to be monitored upon both injection and rinsing in order to extract the same type of kinetic information (association and dissociation rates). The concept here employed is termed *equilibrium fluctuation analysis* [92;97–100] and is based on the ability to monitor biomolecular binding and release events individually. From the statistics of individual bind and release events kinetic information about the biomolecular interaction being studied can then be readily extracted at equilibrium, i.e. without the liquid handling required to control injection and rinsing steps.

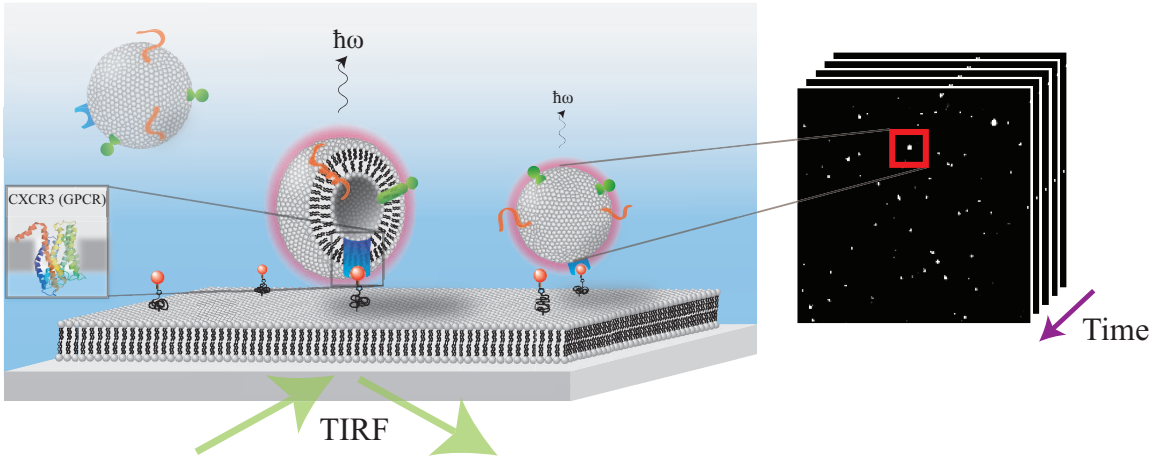

Figure 5.1: *Illustration of the TIRF microscopy assay were chemokine ligands (CXCL10; red spheres) were immobilized on an SLB. Fluorescently labeled native membrane vesicles, expressing the corresponding GPCR receptor (CXCR3; blue), are, when in close proximity to the surface, possible to detect. The low level of unspecific interaction with the underlying SLB and the ability to disregard irreversible interactions this TIRF microscopy assay can be used to characterize the chemokine-GPCR interaction at the level of single interactions.*

Equilibrium fluctuation analysis and a similar TIRF microscopy assay, to the one developed in [92], was employed to determine kinetic parameters describing the interaction between the chemokine receptor CXCR3, belonging to the family of GPCRs, and two of its natural chemokine ligands; CXCL10 and CXCL11. This was realized, as illustrated in figure 5.1, by immobilizing CXCL10 (a small $\sim 9\,\mathrm{kDa}$ protein) on an SLB using a maleimide coupling chemistry [101]. CXCR3 was contained in native membrane vesicles (NMVs) derived from the membrane of CHO-cells [102] genetically modified to overexpress this (human) CXCR3. The membrane of the NMVs was fluorescently labeled via lipid transfer induced by sonication of the NMVs together with synthetically produced fluorescently labeled vesicles [89]. Owing to the TIR illumination, the fluorescent molecules now incorporated into the mem-

brane of the NMVs were only excited once residing in close proximity to the surface, by the evanescent field, where the ligands were present. The receptor-containing NMVs were thus only detected once bound to the immobilized ligands. This is how this concept makes it possible to obtain information about individual ligand-receptor interactions. Thus, the vesicle format both offers a near-native environment for the receptor as well as a possibility to visualize the interaction between the receptor and corresponding ligand via fluorescence but without labeling either of them directly, which might possibly alter the functionality of the proteins[103;104]. The sensitivity offered by the assay format makes it is compatible with low concentrations of membrane receptors, which is particularly interesting in studying GPCRs, that are naturally expressed at low abundance.

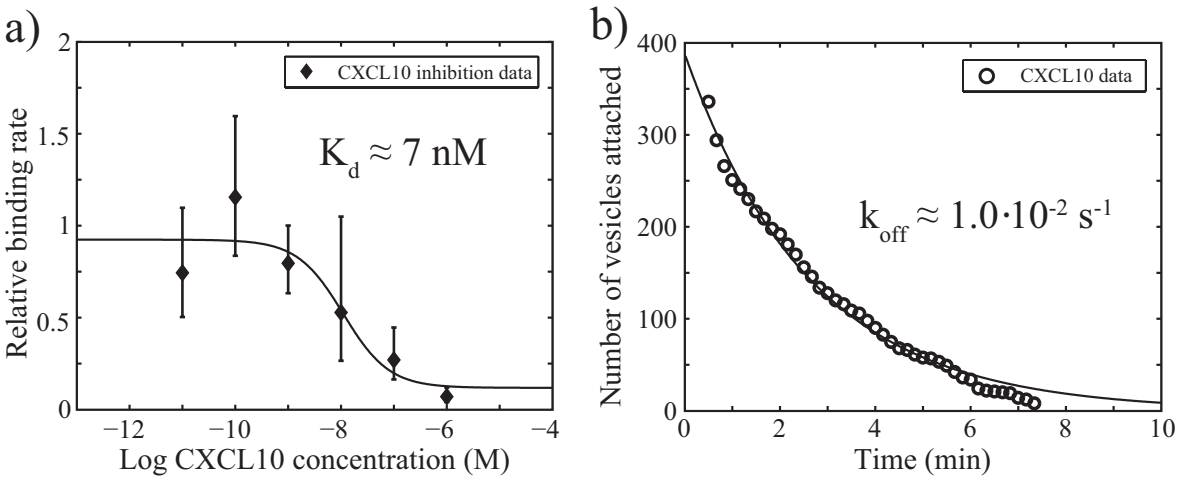

Figure 5.2: ***a***) *Relative binding rate of the fluorescently labeled native membrane vesicles to the surface with immobilized chemokines as free CXCL10 is added in solution at different concentrations inhibiting the interaction. The equilibrium dissociation constant K_d was determined to* $\sim 7\,\mathrm{nM}$. ***b***) *From the residence time of the individual binding events a dissociation curve could be constructed from which the dissociation constant k_{off} was determined. Here, its value was calculated to* $1.0 \cdot 10^{-2}\,\mathrm{s}^{-1}$*, which corresponds to a typical residence time of* $\sim 100\,\mathrm{s}$.

From the TIRF microscopy data of individual NMVs binding and release rates could be readily extracted (see figure 5.2). The affinity (equilibrium dissociation constant) of the interaction was determined by adding free CXCL10 in solution which inhibits the interaction occurring at the surface as fewer CXCR3 receptor become available for binding upon inhibition. In the same way, free CXCL11 was added in solution (still having CXCL10 on the surface), to determine the affinity of the interaction between CXCR3 and CXCL11. In this way we could show that the platform had the capacity of both preserving the function of the GPCR and simultaneously allow for extraction of kinetic information on its biomolecular interactions with specific ligands, which is highly advantageous in discovering and characterizing potential drug molecules targeting GPCRs. The extracted value of the kinetic parameters compare well with those previously reported[105;106].

5.2 Paper II

In the second paper we contributed by developing a surface-based dual-color colocalization assay for verifying a specific interaction between the human cytomegalovirus (HCMV), belonging to the family of herpesviruses, and the membrane protein endothelin B receptor (ETBR), which belongs to the family of GPCRs. Verifying this interaction was a step towards further understanding how HCMV infects endothelial cells (expressing ETBR). To achieve this, as is illustrated in figure 5.3, the enveloped HCMV was fluorescently labeled with a red membrane-inserting dye and attached to an SLB via cholesterol-modified DNA [107;108]. Subsequent addition of green-labeled proteoliposomes containing the ETBR enabled validation of a specific interaction by investigating the degree of spatial overlap between the two entities, i.e. the colocalization level, on the surface.

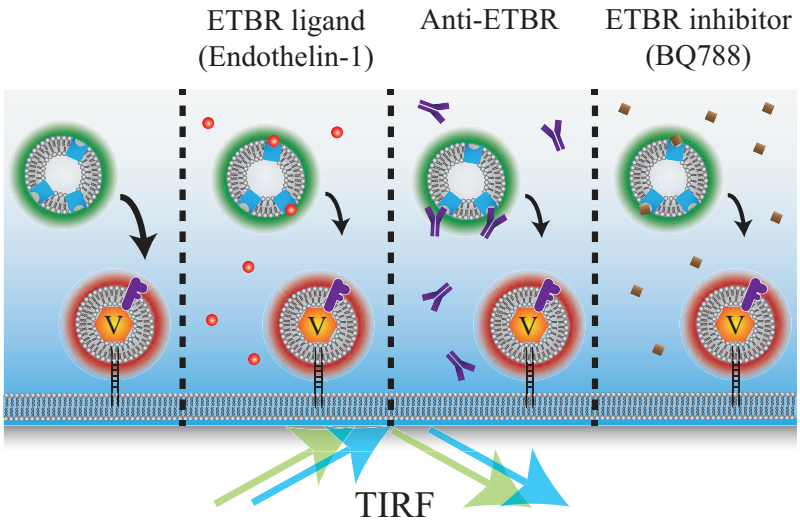

Figure 5.3: *Illustration of how a TIRF-based dual-color colocalization assay was used to verify the specific interaction between ETBR and HCMV. Red-labeled HCMV was immobilized on the SLB via cholesterol-modified DNA. Green-labeled proteoliposomes, containing the ETBR, were introduced in solution and the amount of colocalization was determined. Three different ways of inhibiting the ETBR/HCMV interaction were used to elucidate its specificity.*

The primary parameter assessed in this assay was the degree of colocalization per sensor element, which simply reflects the fraction of immobilized HCMV (red) colocalized with at least one ETBR-proteoliposome (green). To evaluate the specificity of the HCMV/ETBR interaction the colocalization level was also determined after inhibition in three different ways; with ligands (Endothelin-1), antibodies (Anti-ETBR), and inhibitors (BQ788), all directed against the ETBR residing in the proteoliposome.

The outcome of the dual-color colocalization assay is summarized in figure 5.4a, showing micrographs from the red channel, imaging immobilized HCMV, and the green channel, imaging ETBR-proteoliposomes, along with an overlay of the two channels. In the overlay

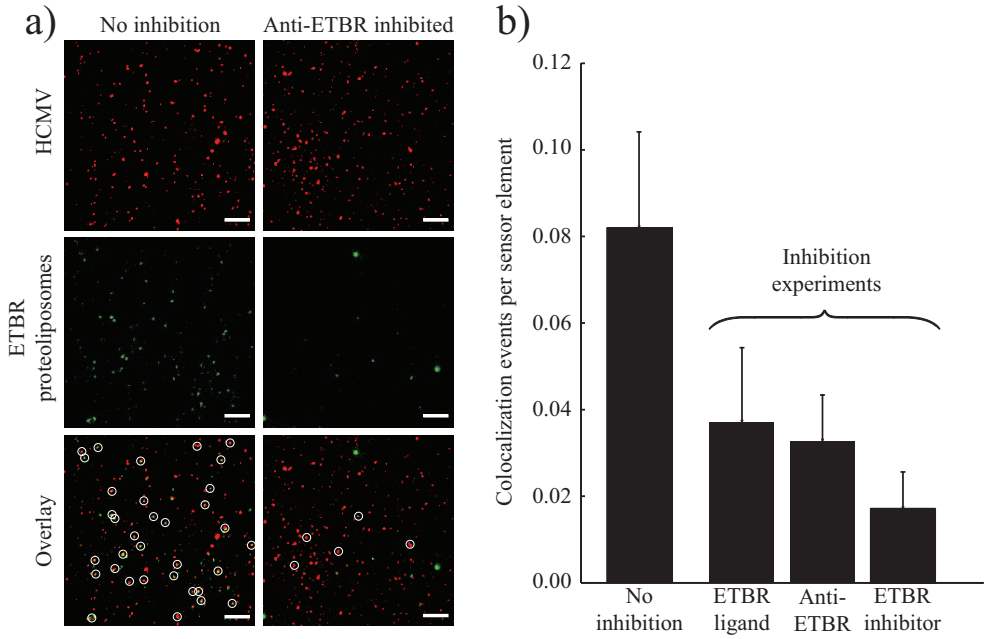

Figure 5.4: *Qualitative and quantitative results from the colocalization assay to verify the physical interaction between ETBR and HCMV.* ***a****) Micrographs (without inhibition and with antibody inhibition) showing red-labeled HCMV (top row), green-labeled ETBR proteoliposomes (middle row) and the corresponding overlays (bottom row). The dots overlapping, termed colocalization events, are marked with white rings for clarity. Scale bars are* 25 μm. ***b****) Number of colocalization events per HCMV bound to the surface for the four different studies. Presented here are mean values* $\pm$ *standard deviations* ($n \geq 3$).

colocalization events are registered, and marked with circles if the centroid position of an ETBR-proteoliposome (green) is within $\sqrt{2}$ pixels (∼500 nm) away from the centroid position of an immobilized HCMV (red). The figure also shows an experiment where an antibody against ETBR was used to inhibit the interaction between the suspended ETBR-proteoliposomes and the HCMV on the surface. As seen in the overlay, the number of colocalization events was significantly reduced upon inhibition. Figure 5.4b shows the quantitative results of the number of colocalization events per visible HCMV (called sensor element) for the four different experiments illustrated in figure 5.3. There is a 2 to 5-fold reduction in colocalization in presence of inhibitors. However, it is clear that all three inhibiting entities decrease the amount of interaction between the HCMV and the ETBR, which strongly indicates that the interaction between them is specific.

Note, however, that even though the assay could confirm a physical interaction between the HCMV and the ETBR it was neither capable of verifying viral entry nor elucidating which part of the virus protein pentamer (on the HCMV) that is responsible for the interaction with the ETBR. Furthermore, it is worth noting that with ETBR being identified as a potential target for antiviral therapy, the surface-based assay developed in this work could aid in future drug-discovery efforts.

5.3 Paper III

In the third paper we developed a solution-based bioanalytical assay for detection of phospholipase A2 (PLA2). Deviations in PLA2 activity and expression level is known to correlate with several different pathological diseases such as cancer[11;12], acute pancreatitis[13], coronary heart disease[14], ischemic stroke[14] and a broad range of neurodegenerative disorders, such as schizophrenia[109] and Alzheimer's disease[110]. For this reason PLA2 concentration and activity can accordingly serve as a diagnostic and prognostic disease biomarker, and has also emerged as a potential target for drug development.

The developed assay exploits the hydrolytic effect of PLA2 to destabilize synthetically produced liposomes and cause them to exchange lipids. Lipid transfer was detected by having the membranes of half of the liposomes labeled with donor fluorophores, and the membranes of the other half labeled with acceptor fluorophores belonging to an established FRET pair, which upon lipid mixing leads to an increased FRET signal. The detection scheme we envisage is illustrated in figure 5.5.

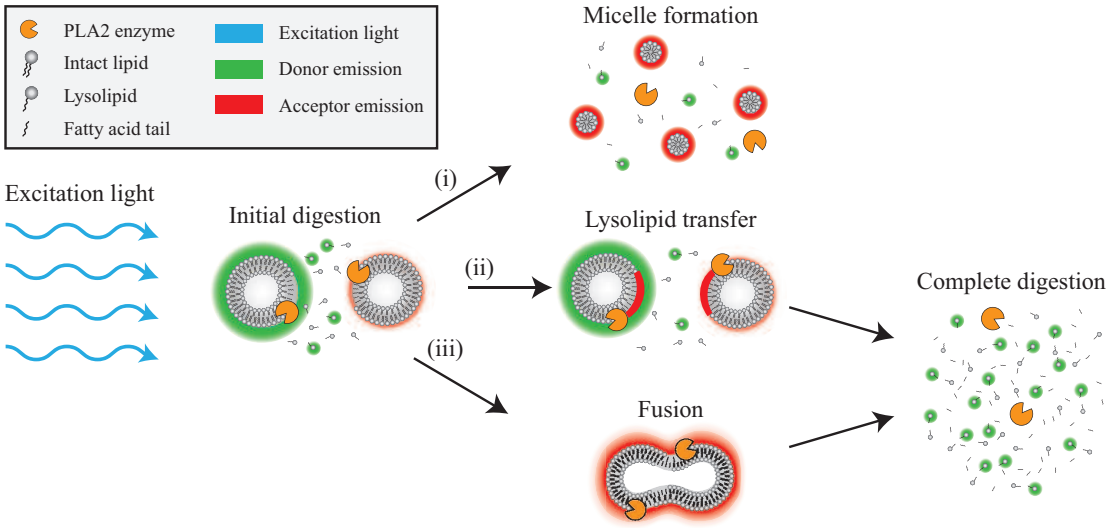

Figure 5.5: *Schematic illustration of detection of PLA2 via lipid mixing between two types of fluorescently labeled liposomes (FRET pair). Upon binding of PLA2 to a liposome the hydrolysis of individual lipids may result in exposure of hydrophobic regions on the liposome surface, which promotes lipid transfer and/or fusion. Lipid mixing results in an increased FRET signal (red color). At complete lipid hydrolysis, the lipid assemblies (not micelles) disintegrate completely and the FRET signal vanishes.*

The possibility to detect PLA2 via FRET induced by lipid mixing via any of the proposed mechanisms (see figure 5.5) was first evaluated using a conventional spectrofluorometer. Liposomes containing donor-conjugated lipids (depicted as green) consisted of POPC and 2wt% DOPE-ATTO488, and the liposomes containing acceptor-conjugated lipids (depicted as faintly red) consisted of POPC and 2wt% DOPE-ATTO633. This fluorophore concen-

tration corresponds to around 1mol% of labeled lipids. For the fluorometer measurements 1 pM of each liposome type was used for PLA2 detection. Figure 5.6a shows how the acceptor emission (at 645 nm) increases upon addition of PLA2. After a certain time the FRET complexes are digested to a state that does not induce FRET at a faster rate than they are created, which makes the acceptor emission decline and eventually stabilize.

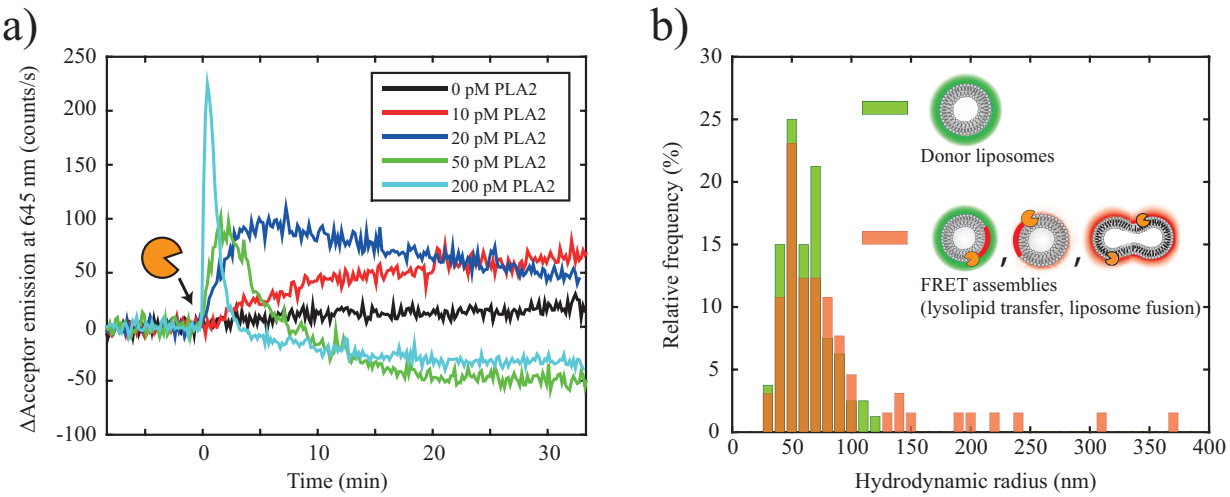

Figure 5.6: ***a***) *Change in acceptor emission (at 645 nm) monitored for a sample of 1 pM donor liposomes and 1 pM acceptor liposomes upon addition of different concentrations of PLA2 measured with spectrofluorometry. A higher enzyme concentration is accompanied by a higher rate of FRET complex formation, but also a faster digestion process after which the FRET signal vanishes.* ***b***) *Size distribution of individual donor liposomes (green) and FRET assemblies (red) extracted from single particle tracking analysis using dual-color fluorescence microscopy.*

To evaluate the molecular mechanism that contributes to the initial increment in the FRET signal and subsequent decline, a dual-color fluorescence microscopy setup was used to image the liposome sample upon addition of PLA2. With an image splitter separating the emission from the donor and acceptor to two adjacent regions on the same camera, the setup offers the possibility to image individual donor liposomes and lipid assemblies (exhibiting FRET) separately. During the digestion process it was evident that individually detectable FRET-active assemblies emerged in the acceptor channel. We also used single particle tracking analysis[111] to determine the hydrodynamic sizes of the visible objects, in each channel respectively (figure 5.6b), demonstrating the appearance of aggregates significantly larger than individual liposomes. However, the majority of the FRET-active assemblies have a size that is comparable to the original size, suggesting that lipid transfer is the dominating source to the observed FRET signal.

5.4 Paper IV

In the fourth paper an assay for selective detection of miRNA based on DNA-mediated liposome fusion was developed. The detection scheme relies on liposomes carrying cholesterol-terminated double-stranded DNA (ds-DNA) that can hybridize together in a zipper-like manner[88;112;113] if a blocking hairpin strand is removed, as is illustrated in figure 5.7. The hairpin is carefully designed to be specifically recognized by the target miRNA and being displaced upon their hybridization. With the blocking strand removed the DNA sequences presented on the two liposome types can hybridize, leading to docking and subsequent fusion between the liposomes. Having one of the liposomes fluorescently labeled with donor fluorophores (DiI) and the other with acceptor fluorophores (DiD) liposome fusion, accompanied by lipid mixing, was detected by a FRET signal increment.

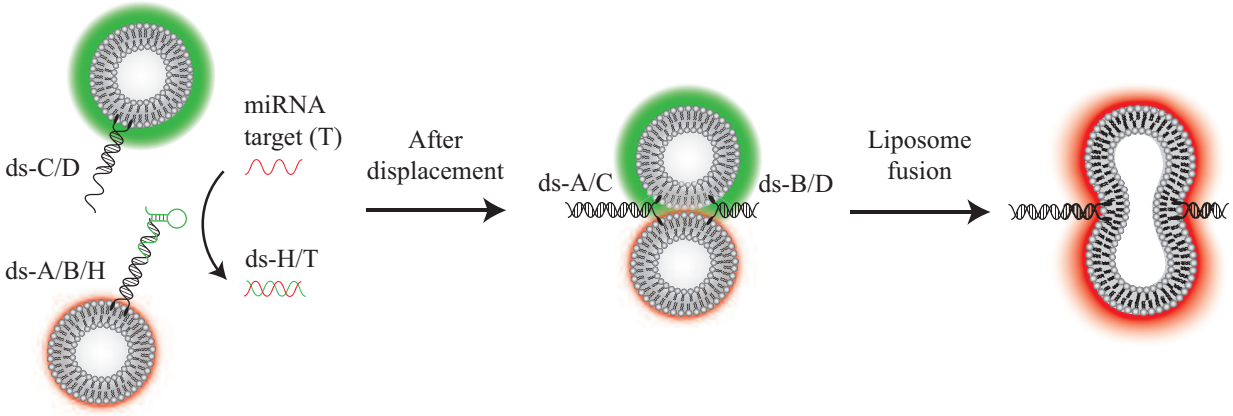

Figure 5.7: *Schematic illustration of the miRNA detection scheme exploiting DNA-mediated liposome fusion. The target miRNA (T: red strand) present in solution is complementary to the hairpin (H: green strand), and upon their hybridization the end of the ds-A/B is revealed. With the hairpin displaced, ds-A/B and ds-C/D hybridize upon contact in a zipper-like manner that promotes liposome fusion accompanied by lipid mixing which results in an increased FRET signal.*

The concept was first verified as very robust and selective using a regular microplate reader. For example, target miRNA designed with only one mismatch resulted in no significant increment in the FRET signal, while the matching miRNA induced a detectable FRET signal with a miRNA concentration down to $\sim 1\,\mathrm{nM}$. Our contribution to this work was to employ the same miRNA detection scheme in the dual-color fluorescence microscopy setup with the intention to lower the limit of detection and the sample consumption. With the dual-color microscopy setup individual donor liposomes and fusion complexes exhibiting FRET could be imaged separately. The intensity traces from the two fluorescence channel are shown in figure 5.8; separated in figure a) and as a ratio in figure b).

Due to a small level of bleed-through from the green to the red channel, in combination with the majority of the detected liposomes being donor liposomes, we were not able to correlate

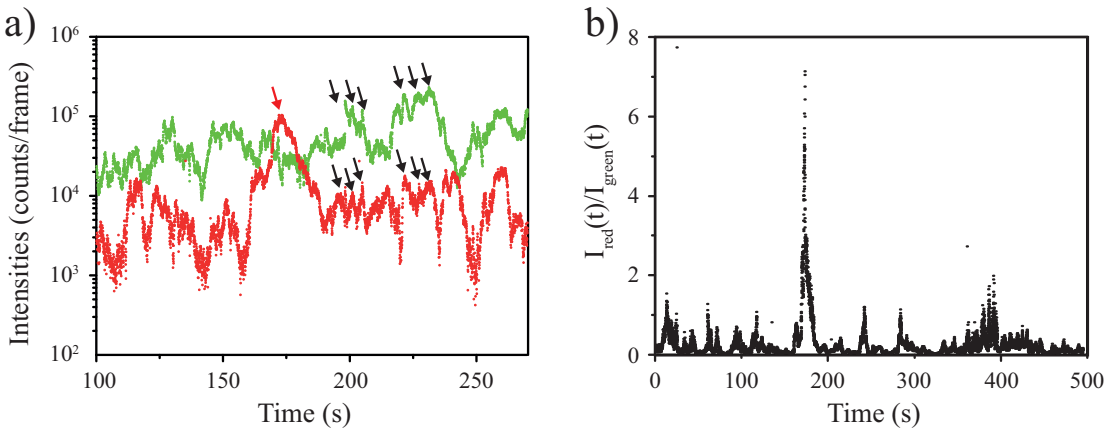

Figure 5.8: ***a***) *Intensity traces over the entire green and red channel, respectively, from the dual-color fluorescence microscopy setup. The fluctuations are caused by donor liposomes (black arrows) and fused liposomes exhibiting FRET (red arrow) entering and leaving the field of view.* ***b***) *Ratio between the red channel intensity, $I_{red}(t)$, and the green channel intensity, $I_{green}(t)$. The burst in the signal are indicative of fused liposomes exhibiting FRET entering the field of view.*

the number of liposome complexes exhibiting FRET with the miRNA concentration in a stringent way. However, the intensity ratio between the two channels, see figure 5.8b, was less sensitive to bleed-through and instead emphasized the events originating from FRET. By applying an autocorrelation formalism, resembling that used in fluorescence correlation spectroscopy (FCS)[114], more accurate results were obtained. The autocorrelation $g(\tau)$, defined as in equation (5.1), was calculated for $I_{red}(t)/I_{green}(t) - \gamma$ (with $\gamma = 0.065$ being the average bleed-through factor).

$$g(\tau) = \frac{\langle I(t) \cdot I(t+\tau) \rangle}{\langle I(t) \rangle^2} - 1 \tag{5.1}$$

Representative autocorrelation functions are shown in 5.9a for three different miRNA concentrations. Here, it is evident that the value of $g(0)$ increases with decreasing miRNA concentration, which is a direct consequence of the number of FRET complexes being fewer as $g(0) = 1/N_{FRET}$. By measuring the corresponding $g(0)$ values for a set of samples with known concentrations of FRET complexes a calibration curve was obtained (not shown) that enabled us to translate the measured $g(0)$ values to FRET complex concentration. The results are shown in figure 5.9b.

With the autocorrelation analysis of the dual-color fluorescence microscopy data we were able to lower the limit of detection by one order of magnitude and the sample consumption by three orders of magnitude.

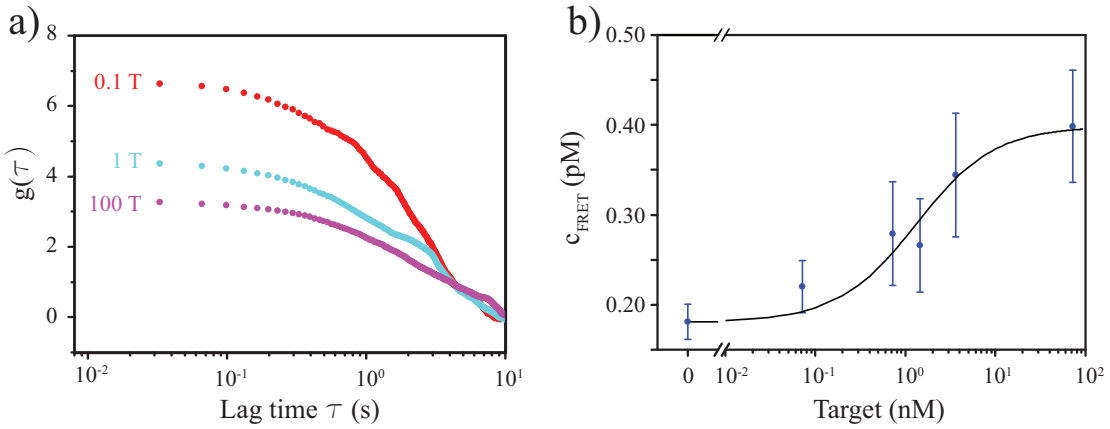

Figure 5.9: ***a***) *Representative autocorrelation functions of* $I_{red}(t)/I_{green}(t) - \gamma$ *(with* $\gamma = 0.065$ *being the average bleed through factor) for three different miRNA concentrations. Here, 1 T corresponds to* $7.2 \cdot 10^{-10}$ M. ***b***) *Dose-response curve with extracted* $g(0)$ *values translated to a corresponding concentration of FRET complexes, here averaged over three independent samples.*

5.5 Paper V

In the fifth paper an assay based on aggregation of fluorescently labeled liposomes was developed for easy, rapid and sensitive detection of SV40 virus-like particles (VLPs). Since typical VLPs are spherical objects with multiple evenly distributed receptor sites, a detection principle based on binding induced colocalization is expected to be generic, while the biological components required for a given virus will be very specific. The idea with the assay is that color-coded reporters, here fluorescently labeled liposomes, carrying a ganglioside specific towards the VP1 protein (360 copies) constituting the capsid of SV40 VLPs[115;116], upon binding to the target can reveal its presence, see figure 5.10. By having half of the liposomes labeled green and half red this assay has an early onset compared to regular aggregation assays, based on for example turbidity, as it is sufficient (in 50% of the cases) to only have two liposomes attached to a VLP for detection.

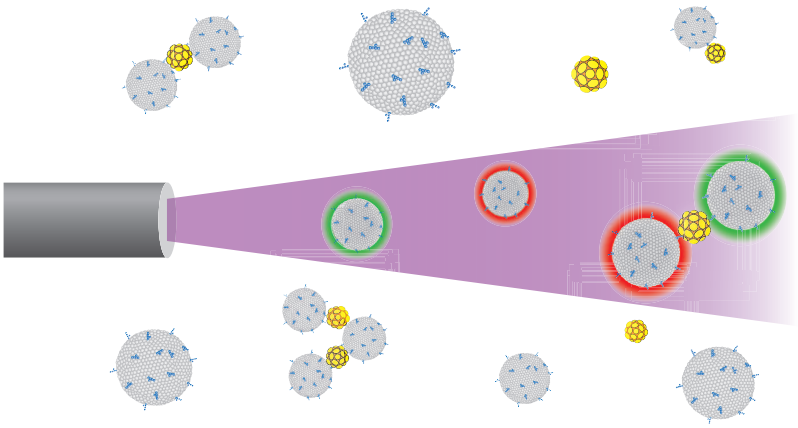

Figure 5.10: *Illustration of how fluorescently labeled (green and red) liposomes, both excited by the light from the optical fiber (two wavelenghts), were used to detect SV40 VLPs in solution. Green and red liposomes, all decorated with the ganglioside GM1 capable of binding to the VP1 proteins constituting the capsid of SV40 VLPs, are diffusing around freely in solution. Upon bridging of at least two differently colored liposomes, by a VLP, complexes are formed that are visible at the same position in both the green and the red emission channel simultaneously, so called colocalization events.*

Dual-color fluorescence microscopy was used to image the sample. With an image splitter the red and green liposomes could be imaged separately. By overlaying the two channels the level of colocalization could be determined. A side note here is that we tried to quantify the colocalization level with the method described in[117] without any significant improvement. Figure 5.11a shows the time-evolution of the colocalization level for a sample with a total liposome concentration of 6.7pM and VLP concentration of 300pM. The sample was diluted 10 times before measuring, to avoid too many fluorecent liposomes being present in the field of view, which would have complicated the analysis. Figure 5.11b shows the colocalization level after 90 min incubation for a range of different SV40 VLP concentrations. The same

liposome concentration and dilution factor was used as in figure 5.11a. As can be seen the colocalization level starts off small, but increases with higher VLP concentration. However, at even higher VLP concentrations the level of colocalization becomes smaller again. This effect is ascribed to the high-dose Hook effect[118], which in this context means that the VLP concentration is so high that individual liposomes are completely coated with VLPs before they get the chance to form bigger aggregates.

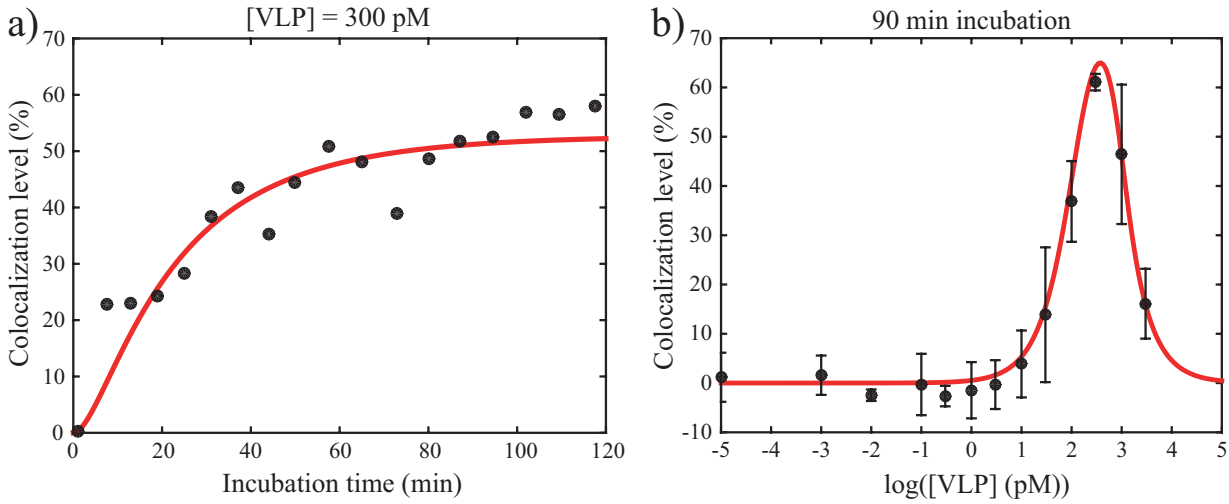

Figure 5.11: ***a***) *Colocalization level over time for a mixture of 6.7 pM liposomes and 300 pM VLP (diluted 10 times when measuring).* ***b***) *Dose-response curve measured after 90 min incubation. The highest colocalization level, around 60-70%, is reached at a VLP concentration of 300 pM. The data points are presented as mean values and the error bars represent the standard deviation (n=3). The fits (solid lines) originate from the theoretical model.*

Further, a theoretical model was formulated that conform well with experimental data presented in figure 5.11. The model was formulated as a set of differential equations, one equation for each individually defined entity in the system, each describing how the concentration of the corresponding entity changes in time i.e. its time-derivative. Since the change in concentration of any entity is most often accompanied by a change in the concentration of other entities the set of differential equations are coupled. By solving the system of coupled differential equations numerically the concentration (time-resolved) of each entity could be extracted. The colocalization level was then readily determined from combinatorics since an aggregate needs to hold at least one liposome of each color to be defined as a possible colocalization event.

With this quantitative bioanalytical assay a virus particle concentration in the 10 pM range was detected within 30 min. The fluorescent liposomes add versatility to the strategy as they can host many different biological molecules (such as for example membrane proteins, DNA, and antibodies) used to recognize and bind to various analytes. The fluorescence readout also enables molecular detection in crude body samples as long as the unspecific interaction with the reporter liposomes is negligible.

6

Concluding remarks and outlook

One of the objectives of the work presented in this thesis was to develop bioanalytical assays compatible with GPCRs, a class of important membrane proteins able to sense changes in the external environment of the cell and convey this information to the cell's interior. Because of this capacity, GPCRs receive significant attention by for example the pharmaceutical industry as suitable targets for new drugs. However, GPCRs are very sensitive to the lipid membrane environment in which they reside, making it challenging to assess them with conventional bioanalytical techniques without risking damage or altering their function.

In **papers I** and **II** two surface-based assays were developed, that take advantage of having the GPCRs incorporated in liposomal structures (either in the form of native membrane vesicles or as proteoliposomes) to maintain a near-natural environment and increase the likelihood of preserving their function. The strategies turned out to be successful, as verified using TIRF microscopy which was used to study the interactions of interest: both GPCR-ligand and GPCR-virus interactions. Even though the methods developed could in principle be used for studying native GPCRs, genetic modifications for overexpression of the GPCRs were used in both cases. GPCRs are low-abundant which makes it challenging, yet still important, to be able to investigate them in their endogeneous state. In section 6.1 we discuss if the method presented in **paper I** can be used to study GPCRs under natural expression levels, which can possibly have great implications for future personalized health care as cellular samples from different individuals will be directly compatible with such analysis methods.

The surface-immobilization of a water soluble ligand employed in **paper I** is not easily translated to study the interactions between a virus particle and a membrane residing membrane protein, since the latter can not be easily distributed on a sensor surface on for example a planar supported lipid bilayer. In **paper II**, we therefore employed a colocalization strategy to be able to more accurately verify a physical interaction between the GPCR and the membrane-enveloped virus (HCMV). To achieve this, an assay was developed where both entities were labeled with different fluorophores and having the virus immobilized on the surface. The specific binding of a proteoliposome (originally in suspension) to a virus

could then be verified by identifying the overlap between the two fluorescent entities. Also, by identifying proteoliposomes that were not overlapping with a virus, originating from unspecific interactions with the surface, these could be disregarded.

With the insights gained from **papers I** and **II** regarding the significant efforts that had to be invested to eliminate non-specific interactions with the underlying surface, the focus of the thesis was shifted towards developing a solution-based bioanalytical assay that could potentially circumvent such problems of unspecific interactions with the underlying substrate while still offering single-molecule sensitivity and possibly low limits of detection.

A new technique, termed dual-color fluorescence microscopy (section 4.4), was developed to enable studies of nanoparticle systems in solution. This technique was successfully implemented for detection of biomarkers (**papers III** and **IV**) and virus particles (**paper V**). For detection of biomarkers, the assays were designed such that FRET was induced among fluorescently labeled liposomes in the presence of the biomarker, while the virus detection instead relied on induced colocalization between fluorescently labeled liposomes. The colocalization method in particular demonstrates promising results and might be adapted for detection of other biomolecules at very low concentrations. Section 6.2 describes how this method, realized in the dual-color fluorescence microscopy setup, should be possible to optimize further to achieve an even better performance. Three improvements, each given a separate subsection, relate to: i) improved sample chamber design, ii) reduction of unspecific interactions between suspended liposomes, and iii) improved image analysis.

6.1 Non-overexpressed GPCR systems

Based on the methods presented in **papers I** and **II** and their compatibility with GPCRs, a collaboration with the department of Microbiology and Immunology at the University of Gothenburg was initiated. They managed, based on fluorescence-activated cell sorting (FACS)[119] measurements, using a fluorescent antibody specific to mouse CXCR3, to identify a mouse cell line (CTLL-2) that naturally expressed CXCR3. Cells from the CTLL-2 cell line were then cultured, harvested and extruded in our lab, to form so-called native membrane vesicles out of the cell membranes. The same strategy as in **paper I** was then employed to investigate if the receptor and corresponding ligand could be studied in a similar way and if the interaction was specific. In brief, the mouse CXCL10 ligand was immobilized on an SLB via a maleimide-based connection chemistry and the QCM-D response was compared between two surfaces, one with ligand present and one without, otherwise identical, upon addition of CTLL-2 vesicles, see figure 6.1. A response of $\Delta f \sim -3.5\,\mathrm{Hz}$ with the ligands present, compared to a response of $\Delta f \sim -0.5\,\mathrm{Hz}$ without the ligands present, gives a promising indication of a specific interaction between the receptor and the ligand.

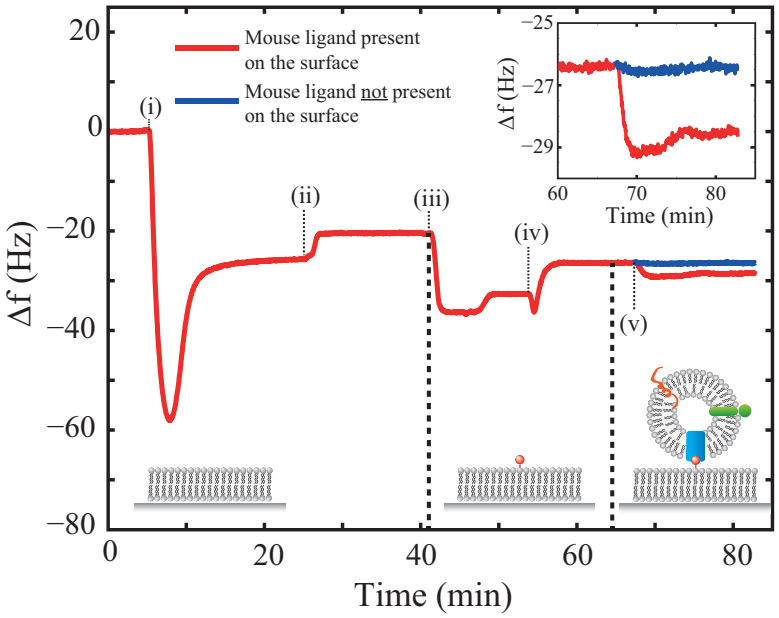

Figure 6.1: *QCM-D plot showing the specific interaction between mouse CXCR3 (receptor) and immobilized mouse CXCL10 (ligand); (i) Injection of POPC + 10%DOPE-MCC (*0.1 mg/ml*) and subsequent bilayer formation, (ii) NaAc (10 mM at pH 5.0) buffer step, (iii) Addition of ligands pre-incubated in Traut's reagent (molar ratio 1:60 at* 100 μg/ml*) and subsequent rinsing with NaAc buffer, (iv) PBS buffer step and, (v) injection of (unlabeled) CXCR3-containing CTLL-2 vesicles. The red curve represents the surface containing ligands and the blue curve a surface with no ligands. Step (v) is emphasized in the upper right inset.*

However, verifying that vesicles derived from the membrane of CTLL-2 cells naturally expressing mouse CXCR3 interact with a surface with immobilized mouse CXCL10 is just the first step in assessing whether the method presented in **paper I** can be employed to study non-overexpressed GPCR systems. The next step would be to confirm that the interaction between CXCR3 and CXCL10 is specific. This could for be done example by inhibiting the interaction by adding free CXCL10 in solution and measuring the resulting response. After verifying that the interaction is indeed specific, TIRF microscopy studies can be performed to try to extract information about individual ligand-receptor interactions and kinetics.

The ability to study non-overexpressed GPCR systems has great benefits for future personalized health care. For example, without the need for overexpression, cells from patients can be directly processed and binding information about the specific GPCR for each patient, with all individual variations and interaction heterogeneities, can be extracted separately. From a future perspective, this paves the way for individually tailored drugs and a more personalized health care.

6.2 Improvements of the colocalization assay

Using colocalization of fluorescently labeled liposomes, decorated with gangliosides, for detection of virus particles directly in solution, as described in **paper V**, is in my view a promising concept that can be further extended. Although many pathogens have membrane bound molecules as natural receptors, the assay could become more generic and allow for detection of other relevant biomolecules and biomarkers by designing the liposomes differently, for example through decoration with antibodies. However, before new ideas are put to the test, there are a few more or less simple ways of improving the dual-color fluorescence microscopy setup and the colocalization experiments and analysis, that should increase both specificity and sensitivity, which is important to make the method more competitive in several different application areas.

6.2.1 Thin sample channel with flow

In the work leading up to **papers III**, **IV** and **V**, dual-color fluorescence microscopy was used. The solution-based measurements were performed in a similar way to that shown in figure 6.2a. The basic setup allows for monitoring of the nanoparticles in (or close to) the focal plane of the objective, which is illuminated by a slightly diverging laser. Particles a bit outside the focal plane (still being illuminated) are captured as fuzzy out-of-focus objects that are difficult to both quantify properly and track, and they might even disturb the detection and analysis of the particles in focus.

To circumvent the problem with out-of-focus particles a thin channel ($\sim 10\mu m$ in height and $\sim 100\mu m$ in width) can be designed, where all particles are forced to pass the field of view close to the focal plane, as is shown in figure 6.2b. Adapting the channel dimensions to ensure that all particles in the channel are detected as focused objects is beneficial in terms of pressing the limit of detection even further down. Thus, if a target molecule of interest is present (and has induced colocalization between liposomes) it will pass the field of view and hence be detected. However, possible problems with background scattering in this configuration might be met by using CYTOP (with a refractive index similar to water) as the channel material instead of PDMS[120].

Along the same lines, another aspect to improve the assay is to detect as many particles as possible within the experiment time. In the current setup, the passive diffusion of particles necessitates long experimental runs to detect enough colocalization events to give statistically valid results. This aspect can be met by gently flowing the sample through the channel. In this way, the rate of particles passing the field of view increases, which theoretically lowers the limit of detection of the device and reduces the experiment time.

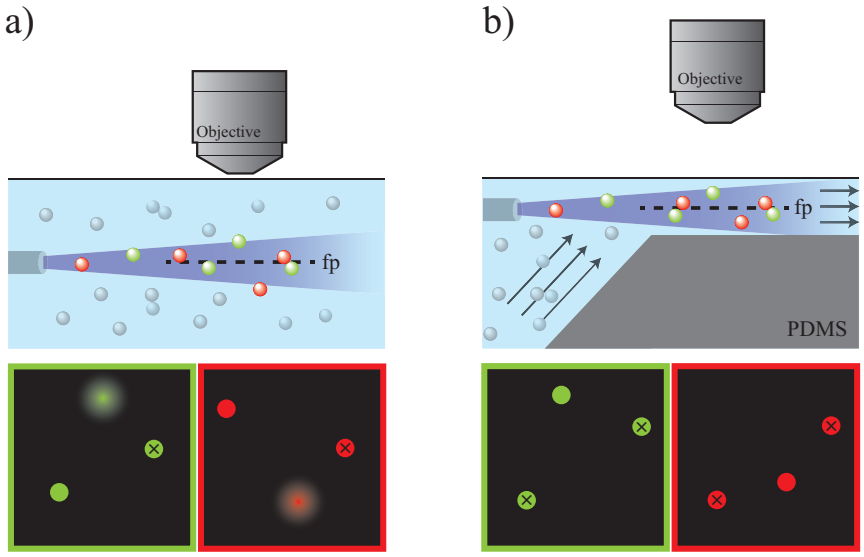

Figure 6.2: ***a***) *Current setup where liposomes in (or close to) the focal plane (fp) are imaged. When liposomes are a bit further away from the focal plane they become unfocused and fuzzy, schematically illustrated in the lower part of the figure. Particles with crosses indicate colocalizing particles.* ***b***) *Proposed modification of the setup where the channel is made thinner (both width and height) to ensure that all particles pass the field of view, and that they are close to the focal plane (fp), as the schematic micrographs below illustrates. Flowing the sample (indicated by the arrows) allows more particles to be imaged within a shorter experiment time.*

6.2.2 Low unspecific interaction

Another important aspect for improving the colocalization assay is to minimize the unspecific interaction between the reporter liposomes. This is because the level of spontaneous colocalization in absence of the target analyte dictates the limit of detection for the assay. A common strategy to minimize unspecific interaction and to passivate surfaces in biosensing application is to use polyethylene glycol (PEG) [121]. In the colocalization assay, decorating the reporter liposomes with a sufficient amount of PEG, as is illustrated in figure 6.3, could aid in lowering the level of spontaneous colocalization and thus improve the limit of detection. However, care needs to be taken that this procedure does not hinder or obstruct the biomolecular interaction that is meant to induce colocalization.

As previously stated the level of spontaneous colocalization in absence of target analyte dictates the limit of detection of the assay. As an example, a liposome concentration of 1 pM and spontaneous pair-formation of one in thousand results in a theoretical sensitivity limit in the fM range. However, a low level of spontaneous pair-formation alone does not ensure low limit of detection. Equally important is the analysis method used to quantify the level of colocalization. The analysis needs to be able to distinguish colocalization events, originating from actual pair-formation, from colocalization events originating from

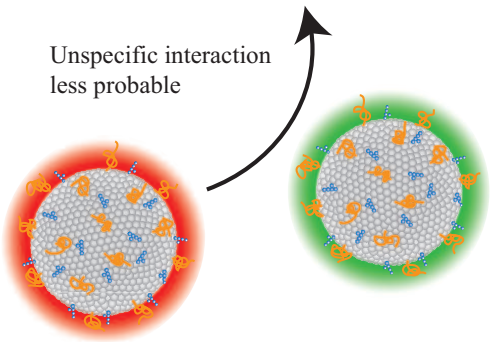

Figure 6.3: *To minimize the level of unspecific interaction between liposomes, they can be decorated with polyethylene glycol (PEG), here depicted as orange coils on the liposome surface.*

liposomes seemingly overlapping at a particular point in time (either due to their immediate vicinity or similar position in the xy-plane, but at different depths (z-value)).

6.2.3 Improved data analysis

In brief, the current image analysis method employed to quantify the colocalization level relies on overlaying the micrographs from the two channels of the image splitter and identifying overlapping objects. Due to chromatic aberration originating from imperfections in the optical system, the overlay has to be carried out in a non-uniform way, through a so-called aberration correction. This correction is carried out computationally by imaging liposomes exhibiting some level of FRET (and hence visible in both channels simultaneously) and mapping their position in the xy-plane. Since the images from the two channels should be perfectly overlapping, a function can be derived that corrects for any misalignment of the objects. This function is then used to map the raw data from a colocalization experiment to yield the correct spatiotemporal position of the objects. However, this method does not account for the fact that the xy-position of two liposomes might occasionally coincide, either because they are found just next to each other (same x-, y- and z-coordinates) by chance or because they are located ”on top” of each other (same x- and y-coordinates, but different z-coordinates), as is schematically shown in 6.4.

The current analysis method that relies on overlaying micrographs, i.e. spatiotemporal overlap, can thus be further improved by also implementing a comparison of liposome trajectories as an additional criteria for verifying colocalization. In brief, individual trajectories of overlapping liposomes must be similar enough for the liposomes to be considered as colocalized. In this way the number of false colocalization events detected would decrease. However, to be able to extract the trajectories with a good enough resolution the acquisition frame rate must be increased considerably, which yields more data to be analyzed for the same experimental time. Here, the aspect of implementing a liquid handling

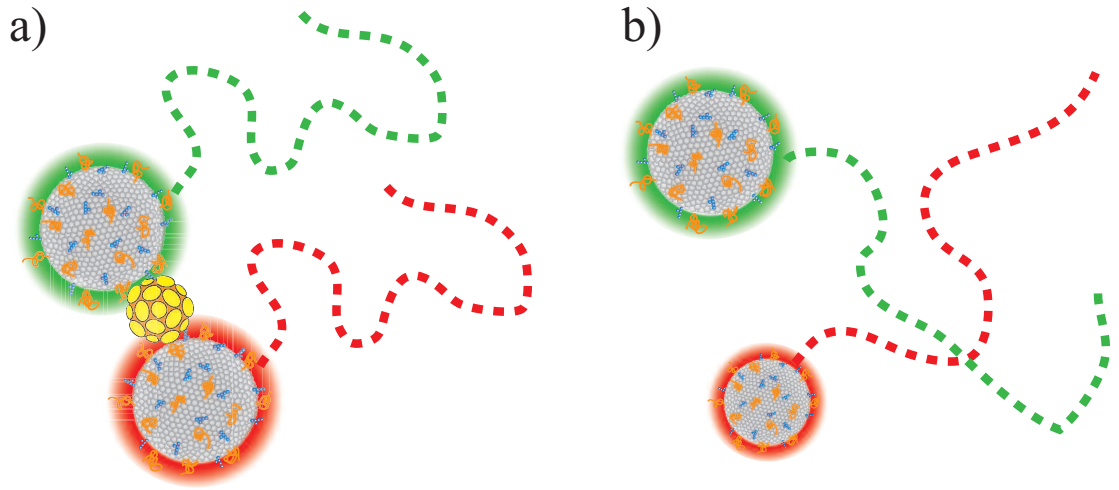

Figure 6.4: *Two different scenarios that with the overlay method are detected as colocalization events.* ***a****) True colocalization event caused by a virus particle bridging a red and a green liposome. The entity moves as a single unit and the separate liposome trajectories are close to identical.* ***b****) False colocalization event where a red and green liposome (not bridged by a virus particle) happen to pass the same point in the xy-plane (either same or not same z-coordinates) at the same time. The liposome trajectories are not similar.*

system with flow becomes relevant as this would be beneficial in terms of detecting many liposomes during the same experimental time.

In light of these three proposed improvements it is important to keep in mind that the theoretical model described in **paper V** is a good complement to the improvements of the experimental setup and the analysis method. Modifications of the theoretical model to account for reversible interactions between the target analyte and the liposomes can deepen the understanding of the performance of the colocalization assay and aid the analysis of targets that do not engage in irreversible binding. This might be valuable for future detection schemes exploiting the strategy of target-induced colocalization of liposomes.

Acknowledgements

I would like to take the opportunity to express my sincerest gratitude to the people contributing to this thesis in one way or the other.

Fredrik Höök, my main supervisor. Your sharp mind, infectious curiosity and witty humour imbue the everyday activities in the group. It surprises me how many astonishing stories you still have up your sleeve. I really appreciate your way of supervising, which is a fine balance between active guidance and spiritual presence.

Anders Gunnarsson and ***Lisa Simonsson Nyström***, my alternating co-supervisors for the beginning of my PhD studies. Thank you so much for all invaluable input to my projects and other issues concerning graduate studies. Also for giving me a broader perspective on academia as well as for occasionally phrasing the short but effectful sentence *"- Bra jobbat, Olov!"*.

Peter Apell. For introducing me to the field of biological physics and for being responsible for the progression of the wound dressing studies initiated already in 2010. Thanks for passing by my office at times to see how things are progressing.

Hudson Pace, my monumental office mate. Thank you for being very supportive, creative, and a great source of inspiration. Also for your frank opinions on several matters. The way I look back at these past years will be strongly impacted by you.

Björn Agnarsson. Your helpfulness, creative mind, and engineering skills have been invaluable to me. Additionally, your Icelandic stoicism, sense of humour, and attitude to work and life is very admirable.

Björn Fast and ***Nadia Peerboom***, precursor and successor in this academic adventure, deserve special mention. Thank you for support and care, all academic advice, the courses we took together, fun times outside of work, and for challenging beer-bets.

All ***Collaborators***. It has been a true pleasure working with you. A special mention goes to ***Frida Ulander***, ***Coline Jumeaux***, and ***Stephan Block***. Your positive attitudes and drive really promotes a creative working environment and steady progress. I wish you the best of luck with your future endeavours, either it being in academia or industry.

Former and present members of the ***Biological Physics group***. For the creative, friendly, and respectful working environment you create.

My Family, ***Bonus Family***, and ***Cecilia*** in particular. For all love, support, encouragement and all the good times.

Olov Wahlsten, Göteborg, July 2017

Bibliography

[1] C. A. Lunn, Membrane proteins as drug targets, Vol. 91, Academic Press, 2010.

[2] M. Guerfal, K. Claes, O. Knittelfelder, R. De Rycke, S. D. Kohlwein, N. Callewaert, Enhanced membrane protein expression by engineering increased intracellular membrane production, Microbial cell factories 12 (1) (2013) 122.

[3] G. Muller, Towards 3d structures of g protein-coupled receptors a multidisciplinary approach, Current medicinal chemistry 7 (9) (2000) 861–888.

[4] P. J. Harding, T. C. Hadingham, J. M. McDonnell, A. Watts, Direct analysis of a gpcr-agonist interaction by surface plasmon resonance, European Biophysics Journal 35 (8) (2006) 709–712.

[5] S. Locatelli-Hoops, A. A. Yeliseev, K. Gawrisch, I. Gorshkova, Surface plasmon resonance applied to g protein-coupled receptors, Biomedical spectroscopy and imaging 2 (3) (2013) 155–181.

[6] B. Vega, A. Calle, A. Sánchez, L. M. Lechuga, A. M. Ortiz, G. Armelles, J. M. Rodríguez-Frade, M. Mellado, Real-time detection of the chemokine cxcl12 in urine samples by surface plasmon resonance, Talanta 109 (2013) 209–215.

[7] N. Bertheleme, S. Singh, S. J. Dowell, J. Hubbard, B. Byrne, Loss of constitutive activity is correlated with increased thermostability of the human adenosine a2a receptor, British journal of pharmacology 169 (5) (2013) 988–998.

[8] J. K. Aronson, Biomarkers and surrogate endpoints, British journal of clinical pharmacology 59 (5) (2005) 491–494.

[9] R. Canfield, S. Birken, J. Morse, F. Morgan, Human chorionic gonadotropin, in: Peptide Hormones, Springer, 1976, pp. 299–315.

[10] U.-H. Stenman, J. Leinonen, W.-M. Zhang, P. Finne, Prostate-specific antigen, in: Seminars in cancer biology, Vol. 9, Elsevier, 1999, pp. 83–93.

[11] S.-I. Yamashita, J.-I. Yamashita, K. Sakamoto, K. Inada, Y. Nakashima, K. Murata, T. Saishoji, K. Nomura, M. Ogawa, Increased expression of membrane-associated phospholipase a2 shows malignant potential of human breast cancer cells, Cancer 71 (10) (1993) 3058–3064.

[12] Z. Dong, Y. Liu, K. F. Scott, L. Levin, K. Gaitonde, R. B. Bracken, B. Burke, Q. J. Zhai, J. Wang, L. Oleksowicz, et al., Secretory phospholipase a2-iia is involved in prostate cancer progression and may potentially serve as a biomarker for prostate cancer, Carcinogenesis 31 (11) (2010) 1948–1955.

[13] T. J. Nevalainen, The role of phospholipase a in acute pancreatitis, Scandinavian journal of gastroenterology 15 (6) (1980) 641–650.

[14] H.-H. S. Oei, I. M. van der Meer, A. Hofman, P. J. Koudstaal, T. Stijnen, M. M. Breteler, J. C. Witteman, Lipoprotein-associated phospholipase a2 activity is associated with risk of coronary heart disease and ischemic stroke, Circulation 111 (5) (2005) 570–575.

[15] H. Song, Q. Wang, Y. Guo, S. Liu, R. Song, X. Gao, L. Dai, B. Li, D. Zhang, J. Cheng, Microarray analysis of microrna expression in peripheral blood mononuclear cells of critically ill patients with influenza a (h1n1), BMC infectious diseases 13 (1) (2013) 257.

[16] R. M. Lequin, Enzyme immunoassay (eia)/enzyme-linked immunosorbent assay (elisa), Clinical chemistry 51 (12) (2005) 2415–2418.

[17] I. Delfino, Light scattering methods for tracking gold nanoparticles aggregation induced by biotin–neutravidin interaction, Biophysical chemistry 177 (2013) 7–13.

[18] N. T. K. Thanh, Z. Rosenzweig, Development of an aggregation-based immunoassay for anti-protein a using gold nanoparticles, Analytical chemistry 74 (7) (2002) 1624–1628.

[19] A. E. James, J. D. Driskell, Monitoring gold nanoparticle conjugation and analysis of biomolecular binding with nanoparticle tracking analysis (nta) and dynamic light scattering (dls), Analyst 138 (4) (2013) 1212–1218.

[20] H. Chen, J.-H. Jiang, Y.-F. Li, T. Deng, G.-L. Shen, R.-Q. Yu, A novel piezoelectric immunoagglutination assay technique with antibody-modified liposome, Biosensors and Bioelectronics 22 (6) (2007) 993–999.

[21] C. A. Mirkin, R. L. Letsinger, R. C. Mucic, J. J. Storhoff, A dna-based method for rationally assembling nanoparticles into macroscopic materials, Nature 382 (6592) (1996) 607–609.

[22] A. Agrawal, R. A. Tripp, L. J. Anderson, S. Nie, Real-time detection of virus particles and viral protein expression with two-color nanoparticle probes, Journal of virology 79 (13) (2005) 8625–8628.

[23] A. Agrawal, C. Zhang, T. Byassee, R. A. Tripp, S. Nie, Counting single native biomolecules and intact viruses with color-coded nanoparticles, Analytical chemistry 78 (4) (2006) 1061–1070.

[24] A. Agrawal, R. Deo, G. D. Wang, M. D. Wang, S. Nie, Nanometer-scale mapping and single-molecule detection with color-coded nanoparticle probes, Proceedings of the National Academy of Sciences 105 (9) (2008) 3298–3303.

[25] J. Liu, X. Yang, K. Wang, Q. Wang, W. Liu, D. Wang, Solid-phase single molecule biosensing using dual-color colocalization of fluorescent quantum dot nanoprobes, Nanoscale 5 (22) (2013) 11257–11264.

[26] S. Gholami, M. Kompany-Zareh, Multiway study of hybridization in nanoscale semiconductor labeled dna based on fluorescence resonance energy transfer, Physical Chemistry Chemical Physics 15 (34) (2013) 14405–14413.

[27] Y.-P. Ho, M. C. Kung, S. Yang, T.-H. Wang, Multiplexed hybridization detection with multicolor colocalization of quantum dot nanoprobes, Nano Letters 5 (9) (2005) 1693–1697.

[28] L. Xiao, L. Wei, Y. He, E. S. Yeung, Single molecule biosensing using color coded plasmon resonant metal nanoparticles, Analytical chemistry 82 (14) (2010) 6308–6314.

[29] T. H. Anderson, Y. Min, K. L. Weirich, H. Zeng, D. Fygenson, J. N. Israelachvili, Formation of supported bilayers on silica substrates, Langmuir 25 (12) (2009) 6997–7005.

[30] J. M. Johnson, T. Ha, S. Chu, S. G. Boxer, Early steps of supported bilayer formation probed by single vesicle fluorescence assays, Biophysical journal 83 (6) (2002) 3371–3379.

[31] R. P. Richter, R. Bérat, A. R. Brisson, Formation of solid-supported lipid bilayers: an integrated view, Langmuir 22 (8) (2006) 3497–3505.

[32] P. Davies, *The fifth miracle: The search for the origin and meaning of life*, Touchstone Books, 2000.

[33] R. Phillips, J. Kondev, J. Theriot, N. Orme, H. Garcia, Physical biology of the cell, Garland Science New York, 2009.

[34] B. Alberts, A. Johnson, J. Lewis, M. Raff, K. Roberts, P. Walter, Molecular biology of the cell (garland science, new york, 2002), There is no corresponding record for this reference.

[35] R. Breslow, Hydrophobic effects on simple organic reactions in water, Accounts of Chemical Research 24 (6) (1991) 159–164.

[36] R. Jones, *Soft Condensed Matter*, Oxford University Press, 2002.

[37] S. J. Singer, G. L. Nicolson, et al., The fluid mosaic model of the structure of cell membranes, Science 175 (23) (1972) 720–731.

[38] M. J. Karnovsky, A. M. Kleinfeld, R. L. Hoover, R. D. Klausner, The concept of lipid domains in membranes., The Journal of cell biology 94 (1) (1982) 1–6.

[39] S. Snogerup Linse, Scientific background on the nobel prize in chemistry 2012 - studies of g-protein–coupled receptors, `http://www.kva.se/globalassets/priser/nobel/2012/kemi/sciback_ke_12.pdf`, accessed: 2014-10-29.

[40] R. Zhang, X. Xie, Tools for gpcr drug discovery, Acta pharmacologica Sinica 33 (3) (2012) 372–384.

[41] R. J. Lefkowitz, Seven transmembrane receptors: something old, something new, Acta physiologica 190 (1) (2007) 9–19.

[42] S. G. Rasmussen, H.-J. Choi, D. M. Rosenbaum, T. S. Kobilka, F. S. Thian, P. C. Edwards, M. Burghammer, V. R. Ratnala, R. Sanishvili, R. F. Fischetti, et al., Crystal structure of the human β_2 adrenergic g-protein-coupled receptor, Nature 450 (7168) (2007) 383.

[43] S. G. Rasmussen, B. T. DeVree, Y. Zou, A. C. Kruse, K. Y. Chung, T. S. Kobilka, F. S. Thian, P. S. Chae, E. Pardon, D. Calinski, et al., Crystal structure of the β_2 adrenergic receptor-gs protein complex, Nature 477 (7366) (2011) 549–555.

[44] D. Massotte, G protein-coupled receptor overexpression with the baculovirus–insect cell system: a tool for structural and functional studies, Biochimica et Biophysica Acta (BBA)-Biomembranes 1610 (1) (2003) 77–89.

[45] P. Stenlund, G. J. Babcock, J. Sodroski, D. G. Myszka, Capture and reconstitution of g protein-coupled receptors on a biosensor surface, Analytical biochemistry 316 (2) (2003) 243–250.

[46] R. D. Schmid, R. Verger, Lipases: interfacial enzymes with attractive applications, Angewandte Chemie International Edition 37 (12) (1998) 1608–1633.

[47] A. Svendsen, Lipase protein engineering, Biochimica et Biophysica Acta (BBA)-Protein Structure and Molecular Enzymology 1543 (2) (2000) 223–238.

[48] R. C. Lee, R. L. Feinbaum, V. Ambros, The c. elegans heterochronic gene lin-4 encodes small rnas with antisense complementarity to lin-14, Cell 75 (5) (1993) 843–854.

[49] J. Wang, S. Sen, Microrna functional network in pancreatic cancer: from biology to biomarkers of disease, Journal of biosciences 36 (3) (2011) 481–491.

[50] J. Wang, J. Chen, S. Sen, Microrna as biomarkers and diagnostics, Journal of cellular physiology 231 (1) (2016) 25–30.

[51] A. Roberts, A. P. Lewis, C. L. Jopling, The role of micrornas in viral infection., Progress in molecular biology and translational science 102 (2011) 101–139.

[52] D. J. Griffiths, Endogenous retroviruses in the human genome sequence, Genome biology 2 (6) (2001) reviews1017–1.

[53] J. Grove, M. Marsh, The cell biology of receptor-mediated virus entry, J Cell Biol 195 (7) (2011) 1071–1082.

[54] S. Miller, J. Krijnse-Locker, Modification of intracellular membrane structures for virus replication, Nature reviews. Microbiology 6 (5) (2008) 363.

[55] J. H. Hurley, E. Boura, L.-A. Carlson, B. Różycki, Membrane budding, Cell 143 (6) (2010) 875–887.

[56] D. M. Addington, D. L. Schodek, Smart materials and new technologies: for the architecture and design professions, Routledge, 2005.

[57] N. Bhalla, P. Jolly, N. Formisano, P. Estrela, Introduction to biosensors, Essays in biochemistry 60 (1) (2016) 1–8.

[58] A. Turner, I. Karube, G. S. Wilson, Biosensors: fundamentals and applications, Oxford university press, 1987.

[59] T. H. Rider, M. S. Petrovick, F. E. Nargi, J. D. Harper, E. D. Schwoebel, R. H. Mathews, D. J. Blanchard, L. T. Bortolin, A. M. Young, J. Chen, et al., Ab cell-based sensor for rapid identification of pathogens, Science 301 (5630) (2003) 213–215.

[60] G. Wang, A. H. Dewilde, J. Zhang, A. Pal, M. Vashist, D. Bello, K. A. Marx, S. J. Braunhut, J. M. Therrien, A living cell quartz crystal microbalance biosensor for continuous monitoring of cytotoxic responses of macrophages to single-walled carbon nanotubes, Particle and fibre toxicology 8 (1) (2011) 4.

[61] W. R. Heineman, W. B. Jensen, Leland c. clark jr.(1918–2005), Biosensors and Bioelectronics 21 (8) (2006) 1403–1404.

[62] K. Tonyushkina, J. H. Nichols, Glucose meters: a review of technical challenges to obtaining accurate results, Journal of diabetes science and technology 3 (4) (2009) 971–980.

[63] J. Wang, Electrochemical glucose biosensors, Chemical reviews 108 (2) (2008) 814–825.

[64] C. Gnoth, S. Johnson, Strips of hope: accuracy of home pregnancy tests and new developments, Geburtshilfe und Frauenheilkunde 74 (07) (2014) 661–669.

[65] H. A. Erlich, Polymerase chain reaction, Journal of clinical immunology 9 (6) (1989) 437–447.

[66] A. P. Turner, Biosensors–sense and sensitivity, Science 290 (5495) (2000) 1315–1317.

[67] J. P. Chambers, B. P. Arulanandam, L. L. Matta, A. Weis, J. J. Valdes, Biosensor recognition elements, Tech. rep., Texas Univ at San Antonio Dept of Biology (2008).

[68] F. Vollmer, S. Arnold, Whispering-gallery-mode biosensing: label-free detection down to single molecules, Nature methods 5 (7) (2008) 591–596.

[69] D. M. Rissin, C. W. Kan, T. G. Campbell, S. C. Howes, D. R. Fournier, L. Song, T. Piech, P. P. Patel, L. Chang, A. J. Rivnak, et al., Single-molecule enzyme-linked immunosorbent assay detects serum proteins at subfemtomolar concentrations, Nature biotechnology 28 (6) (2010) 595–599.

[70] A. Janshoff, H.-J. Galla, C. Steinem, Piezoelectric mass-sensing devices as biosensors - an alternative to optical biosensors?, Angew. Chem. Int. Ed 39 (2000) 4004–4032.

[71] N.-J. Cho, C. W. Frank, B. Kasemo, F. Höök, Quartz crystal microbalance with dissipation monitoring of supported lipid bilayers on various substrates, nature protocols 5 (6) (2010) 1096–1106.

[72] E. Nilebäck, F. Westberg, J. Deinum, S. Svedhem, Viscoelastic sensing of conformational changes in plasminogen induced upon binding of low molecular weight compounds, Analytical chemistry 82 (20) (2010) 8374–8376.

[73] R. P. Richter, K. K. Hock, J. Burkhartsmeyer, H. Boehm, P. Bingen, G. Wang, N. F. Steinmetz, D. J. Evans, J. P. Spatz, Membrane-grafted hyaluronan films: a well-defined model system of glycoconjugate cell coats, Journal of the American Chemical Society 129 (17) (2007) 5306–5307.

[74] N. Tymchenko, E. Nilebäck, M. V. Voinova, J. Gold, B. Kasemo, S. Svedhem, Reversible changes in cell morphology due to cytoskeletal rearrangements measured in real-time by qcm-d, Biointerphases 7 (1) (2012) 43.

[75] R. Frost, E. Norström, L. Bodin, C. Langhammer, J. Sturve, M. Wallin, S. Svedhem, Acoustic detection of melanosome transport in< i> xenopus laevis</i> melanophores, Analytical biochemistry 435 (1) (2013) 10–18.

[76] M. A. Cooper, Advances in membrane receptor screening and analysis, Journal of Molecular Recognition 17 (4) (2004) 286–315.

[77] J. Curie, P. Curie, An oscillating quartz crystal mass detector, Rendu 91 (1880) 294–297.

[78] R. Ebersole, J. Miller, J. Moran, M. Ward, Pz quartz sensors for use in clinical analysis, J. Am. Chem. Soc 112 (1990) 3239.

[79] G. Sauerbrey, Verwendung von schwingquarzen zur wägung dünner schichten und zur mikrowägung, Zeitschrift für Physik 155 (2) (1959) 206–222.

[80] E. Nilebäck, QCM-D–with focus on biosensing in biomolecular and cellular systems, Chalmers University of Technology, 2013.

[81] E. Reimhult, B. Kasemo, F. Höök, Rupture pathway of phosphatidylcholine lipo-

somes on silicon dioxide, International journal of molecular sciences 10 (4) (2009) 1683–1696.

[82] J. R. Lakowicz, Principles of fluorescence spectroscopy (2006).

[83] T. W. Gadella, FRET and FLIM techniques, Vol. 33, Elsevier, 2011.

[84] C. Berney, G. Danuser, Fret or no fret: a quantitative comparison, Biophysical journal 84 (6) (2003) 3992–4010.

[85] B. Schuler, W. A. Eaton, Protein folding studied by single-molecule fret, Current opinion in structural biology 18 (1) (2008) 16–26.

[86] L. M. Loura, M. Prieto, Fret in membrane biophysics: An overview, Frontiers in physiology 2.

[87] H. Robson Marsden, N. A. Elbers, P. H. Bomans, N. A. Sommerdijk, A. Kros, A reduced snare model for membrane fusion, Angewandte Chemie International Edition 48 (13) (2009) 2330–2333.

[88] G. Stengel, L. Simonsson, R. A. Campbell, F. Höök, Determinants for membrane fusion induced by cholesterol-modified dna zippers, The Journal of Physical Chemistry B 112 (28) (2008) 8264–8274.

[89] H. Pace, L. Simonsson Nyström, A. Gunnarsson, E. Eck, C. Monson, S. Geschwindner, A. Snijder, F. Höök, Preserved transmembrane protein mobility in polymer-supported lipid bilayers derived from cell membranes, Analytical chemistry 87 (18) (2015) 9194–9203.

[90] D. K. Struck, D. Hoekstra, R. E. Pagano, Use of resonance energy transfer to monitor membrane fusion, Biochemistry 20 (14) (1981) 4093–4099.

[91] Lipophilic Tracers - DiI, DiO, DiD, DiA, and DiR. https://tools.thermofisher.com/content/sfs/manuals/mp00282.pdf. Retrieved: 2017-07-29.

[92] A. Gunnarsson, L. Dexlin, P. Wallin, S. Svedhem, P. Jönsson, C. Wingren, F. Höök, Kinetics of ligand binding to membrane receptors from equilibrium fluctuation analysis of single binding events, Journal of the American Chemical Society 133 (38) (2011) 14852–14855.

[93] D. Axelrod, T. P. Burghardt, N. L. Thompson, Total internal reflection fluorescence, Annual review of biophysics and bioengineering 13 (1) (1984) 247–268.

[94] Nanoparticle Tracking Analysis - https://www.malvern.com/en/products/technology/nanoparticle-tracking-analysis. Retrieved: 2017-07-30.

[95] R. L. Bunde, E. J. Jarvi, J. J. Rosentreter, Piezoelectric quartz crystal biosensors, Talanta 46 (6) (1998) 1223–1236.

[96] P. Pattnaik, Surface plasmon resonance, Applied biochemistry and biotechnology 126 (2) (2005) 79–92.

[97] A. Gunnarsson, P. Jönsson, R. Marie, J. O. Tegenfeldt, F. Höök, Single-molecule detection and mismatch discrimination of unlabeled dna targets, Nano letters 8 (1) (2008) 183–188.

[98] M. Bally, M. Graule, F. Parra, G. Larson, F. Höök, A virus biosensor with single virus-particle sensitivity based on fluorescent vesicle labels and equilibrium fluctuation analysis, Biointerphases 8 (1) (2013) 4.

[99] A. Kunze, M. Bally, F. Höök, G. Larson, Equilibrium-fluctuation-analysis of single liposome binding events reveals how cholesterol and ca2+ modulate glycosphingolipid trans-interactions, Scientific reports 3.

[100] N. Peerboom, S. Block, N. Altgärde, O. Wahlsten, S. Möller, M. Schnabelrauch, E. Trybala, T. Bergström, M. Bally, Binding kinetics and lateral mobility of hsv-1 on end-grafted sulfated glycosaminoglycans, Biophysical Journal.

[101] M. Brinkley, A brief survey of methods for preparing protein conjugates with dyes, haptens and crosslinking reagents, Bioconjugate chemistry 3 (1) (1992) 2–13.

[102] F. M. Wurm, Production of recombinant protein therapeutics in cultivated mammalian cells, Nature biotechnology 22 (11) (2004) 1393–1398.

[103] R. Sridharan, J. Zuber, S. M. Connelly, E. Mathew, M. E. Dumont, Fluorescent approaches for understanding interactions of ligands with g protein coupled receptors, Biochimica et Biophysica Acta (BBA)-Biomembranes 1838 (1) (2014) 15–33.

[104] Y.-S. Sun, J. P. Landry, Y. Fei, X. Zhu, J. Luo, X. Wang, K. Lam, Effect of fluorescently labeling protein probes on kinetics of protein- ligand reactions, Langmuir 24 (23) (2008) 13399–13405.

[105] I. Clark-Lewis, I. Mattioli, J.-H. Gong, P. Loetscher, Structure-function relationship between the human chemokine receptor cxcr3 and its ligands, Journal of Biological Chemistry 278 (1) (2003) 289–295.

[106] X. Wang, X. Li, D. B. Schmidt, J. J. Foley, F. C. Barone, R. S. Ames, H. M. Sarau, Identification and molecular characterization of rat cxcr3: receptor expression and interferon-inducible protein-10 binding are increased in focal stroke, Molecular pharmacology 57 (6) (2000) 1190–1198.

[107] I. Pfeiffer, F. Höök, Bivalent cholesterol-based coupling of oligonucletides to lipid membrane assemblies, Journal of the American Chemical Society 126 (33) (2004) 10224–10225.

[108] S. Svedhem, I. Pfeiffer, C. Larsson, C. Wingren, C. Borrebaeck, F. Höök, Patterns of dna-labeled and scfv-antibody-carrying lipid vesicles directed by material-specific

immobilization of dna and supported lipid bilayer formation on an au/sio2 template, ChemBioChem 4 (4) (2003) 339–343.

[109] W. F. Gattaz, C. Hubner, T. J. Nevalainen, T. Thuren, P. Kinnunen, Increased serum phospholipase a 2 activity in schizophrenia: a replication study, Biol Psychiatry 28 (6) (1990) 495–501.

[110] S. Chalbot, H. Zetterberg, K. Blennow, T. Fladby, I. Grundke-Iqbal, K. Iqbal, Cerebrospinal fluid secretory ca 2+-dependent phospholipase a2 activity: A biomarker of blood–cerebrospinal fluid barrier permeability, Neuroscience letters 478 (3) (2010) 179–183.

[111] E. Meijering, O. Dzyubachyk, I. Smal, Imaging and spectroscopic analysis of living cells, Methods in Enzymology. Elsevier (2012) 183–200.

[112] G. Stengel, R. Zahn, F. Höök, Dna-induced programmable fusion of phospholipid vesicles, Journal of the American Chemical Society 129 (31) (2007) 9584–9585.

[113] L. Simonsson, P. Jönsson, G. Stengel, F. Höök, Site-specific dna-controlled fusion of single lipid vesicles to supported lipid bilayers, ChemPhysChem 11 (5) (2010) 1011–1017.

[114] E. L. Elson, D. Magde, Fluorescence correlation spectroscopy. i. conceptual basis and theory, Biopolymers 13 (1) (1974) 1–27.

[115] D. M. Salunke, D. L. Caspar, R. L. Garcea, Self-assembly of purified polyomavirus capsid protein vp1, Cell 46 (6) (1986) 895–904.

[116] T. Stehle, S. J. Gamblin, Y. Yan, S. C. Harrison, The structure of simian virus 40 refined at 3.1 å resolution, Structure 4 (2) (1996) 165–182.

[117] S. V. Costes, D. Daelemans, E. H. Cho, Z. Dobbin, G. Pavlakis, S. Lockett, Automatic and quantitative measurement of protein-protein colocalization in live cells, Biophysical journal 86 (6) (2004) 3993–4003.

[118] J. Tate, G. Ward, Interferences in immunoassay, The clinical biochemist reviews 25 (2) (2004) 105.

[119] W. Bonner, H. Hulett, R. Sweet, L. Herzenberg, Fluorescence activated cell sorting, Review of Scientific Instruments 43 (3) (1972) 404–409.

[120] B. Agnarsson, A. Lundgren, A. Gunnarsson, M. Rabe, A. Kunze, M. Mapar, L. Simonsson, M. Bally, V. P. Zhdanov, F. Höök, Evanescent light-scattering microscopy for label-free interfacial imaging: from single sub-100 nm vesicles to live cells, ACS nano 9 (12) (2015) 11849–11862.

[121] H. Du, P. Chandaroy, S. W. Hui, Grafted poly-(ethylene glycol) on lipid surfaces inhibits protein adsorption and cell adhesion, Biochimica et Biophysica Acta (BBA)-Biomembranes 1326 (2) (1997) 236–248.